



1 **Parameterization of the light absorption properties of chromophoric dissolved organic**
2 **matter in the Baltic Sea and Pomeranian Lakes**

3 Justyna Meler^{a*}, Piotr Kowalczyk^a, Mirosława Ostrowska^a, Dariusz Ficek^b, Monika
4 Zabłocka^a, Agnieszka Zdun^a

5 ^a Institute of Oceanology Polish Academy of Sciences, Powstańców Warszawy 55, 81-712
6 Sopot, Poland

7 ^b Institute of Physics, Pomeranian University of Słupsk, Bohaterów Westerplatte 64, 76-200
8 Słupsk, Poland

9 * corresponding author: jmeler@iopan.pl

10

11 Keywords: Baltic Sea; Pomeranian lakes; Chromophoric Dissolved Organic Matter; three
12 alternative models of CDOM absorption; light absorption; ocean optics

13

14 **Abstract**

15 This study presents three alternative models for estimation of absorption properties of
16 Chromophoric Dissolved Organic Matter, $a_{CDOM}(\lambda)$. For this analysis we used a database
17 containing 556 absorption spectra measured in 2006 – 2009 in different regions of the Baltic
18 Sea (open and coastal waters, the Gulf of Gdańsk and the Pomeranian Bay), at river mouths,
19 in the Szczecin Lagoon and also in three Pomeranian lakes in Poland – Lakes Obłęskie,
20 Łebsko and Chotkowskie. Observed variability range of the CDOM absorption coefficient at
21 400 nm, $a_{CDOM}(400)$, contained within 0.15 – 8.85 m^{-1} . The variability in $a_{CDOM}(\lambda)$ was
22 parameterized with respect to three orders of magnitude variability in the chlorophyll *a*
23 concentration *Chla* (0.7 – 119 $mg\ m^{-3}$). Chlorophyll *a* concentration and CDOM absorption
24 coefficient, $a_{CDOM}(400)$ were correlated, and statistically significant, non-linear empirical
25 relationship between those parameters was derived ($R^2=0.83$). Based on observed co-variance
26 between these parameters, we derived two empirical mathematical models that enabled to
27 project the CDOM absorption coefficient dynamics in natural waters and reconstruct the
28 completed CDOM absorption spectrum in the UV and visible spectral domains. The first
29 model used the chlorophyll *a* concentration as the input variable. The second model used the
30 $a_{CDOM}(400)$, as the input variable. Both models were fitted to power function and the second
31 order polynomial function was used as the exponent. Regression coefficients for derived
32 formulas were determined for wavelengths from 240 to 700 nm at 5 nm intervals . Both



33 approximation reflected the real shape of the absorption spectra with low uncertainty.
34 Comparison of these approximation with other models of light absorption by CDOM proved
35 that proposed parameterizations were better (bias from -1.45% to 62%, RSME from 22% to
36 220%) for estimation CDOM absorption in optically complex waters of the Baltic Sea and
37 lakes.

38 1. Introduction

39 All natural waters contain optically significant constituents that determines their
40 inherent optical properties: absorption coefficient, scattering coefficient and beam attenuation
41 coefficient. The total absorption coefficient in ultraviolet and visible spectral range of the
42 electromagnetic radiation spectrum, is almost entirely determined by four main groups of
43 absorbents: water molecules, organic and inorganic suspended particulate matter (SPM), and
44 Chromophoric Dissolved Organic Matter (CDOM). The quantity and qualitative properties of
45 these absorbents significantly affect the quantity and spectral distribution of light in the
46 aquatic environment. The absorption of pure water measured by Pope and Fry (1997) is
47 almost constant in natural waters and may be omitted in further analysis because it does not
48 contribute to a variability of total absorption coefficient. Changes in spectral values of the
49 pure sea water are almost entirely determined by the concentration and the composition of sea
50 salt ions and dissolved gases, and is mostly pronounced in the UV-A and UV-B spectral
51 region below 300 nm (Woźniak and Dera, 2007). Spectral properties (values and spectral
52 shape) and the mutual proportions of light absorption coefficients by CDOM, $a_{\text{CDOM}}(\lambda)$, by
53 phytoplankton pigments, $a_{\text{ph}}(\lambda)$, organic detritus and mineral particles $a_{\text{NAP}}(\lambda)$, determine the
54 spectral shape and magnitude of the total absorption spectrum as well as affects both the
55 inherent and the apparent optical properties of natural waters (Woźniak and Dera, 2007).

56 The Chromophoric Dissolved Organic Matter is the uncharacterized fraction of the
57 dissolved organic matter pool consisting from heterogeneous mixture of water soluble organic
58 compounds that have ability to absorb light (Nelson and Siegel, 2002). The effect of the
59 CDOM absorption is mostly visible in the UV and blue spectral range of electromagnetic
60 radiation, where CDOM contribution to the total non-water absorption could reach 90%, even
61 in the clearest natural waters found in South Pacific Subtropical Gyre south off Easter Island,
62 (Morel et al., 2007; Bricaud et al., 2010; Tedetti et al., 2010). Presence of high concentration
63 of CDOM usually shift the spectral maximum of the water transparency to solar radiation and
64 water leaving radiance toward the longer wavelength (Darecki et al., 2003; Morel and Gentili,



65 2009). In extreme cases, in humic boreal lakes, the CDOM reduces the water leaving radiance
66 intensity in the visible spectrum almost to null (Ficek et al., 2011; Ficek et al., 2012; Ylöstalo
67 et al., 2014). CDOM absorption band overlaps also with primary phytoplankton pigment
68 absorption band in the blue part of the spectrum contributing to significant errors of standard
69 algorithms for retrievals of chlorophyll *a*, especially in coastal ocean and shelf and semi-
70 enclosed seas (Darecki and Stramski, 2004; Siegel et al., 2005). Therefore, appropriate
71 quantitative and qualitative descriptions of the optical properties of CDOM is crucial in the
72 ocean color remote sensing of aquatic environments.

73 CDOM plays also various ecological roles in aquatic environments: even small
74 concentrations strongly absorb UV radiation, protecting organisms from its destructive action.
75 Higher levels of CDOM absorptions limits the amount of radiation available for
76 photosynthesis and consequently reducing the primary production of organic matter in that
77 water (Górniak, 1996; Wetzel, 2001). CDOM plays an important part in various biological
78 processes taking place in water bodies: it can affect the species composition, number and size
79 of plankton organisms (Arrigo and Brown, 1996; Campanelli et al., 2009), and in oligotrophic
80 lakes can promote the growth of bacterioplankton (Moran and Hodson, 1994). Several authors
81 have pointed out that CDOM is a potential source of reactive oxygen forms in aquatic
82 ecosystems, which has a considerable influence on a variety of biological processes
83 (Whitehead and de Mora, 2000; Kieber et al., 2003).

84 CDOM absorption decreases exponentially towards longer wavelengths and can be
85 described by the exponential function (Jerlov, 1976, Bricaud et al., 1981, Kirk 1994):

$$86 \quad a_{CDOM}(\lambda) = a_{CDOM}(\lambda_0)e^{-S(\lambda_0 - \lambda)} \quad (1)$$

87 where: $a_{CDOM}(\lambda)$ is the light absorption coefficient for a given wavelength λ , λ_0 is the
88 reference wavelength, and S is the slope of the spectrum within a given wavelength interval.

89 The CDOM accumulates in the surface Baltic Sea waters as a combined effect very
90 high inflow of fresh water from rivers and the limited exchange of waters with the North Sea
91 and very high productivity of this marine basin, (Kowalczyk et al., 2006). The systematic
92 studies over the last two decades on optical properties in the Baltic Sea waters and adjacent
93 fresh water systems coastal lagoons and Pomeranian lakes, provided evidence that the CDOM
94 is the principal absorbent of solar radiation and the main factor governing their optical
95 properties (Kowalczyk 1999; Kowalczyk et al., 2005; 2006; 2010; Ficek et al., 2012; Ficek
96 2013).



97 The main objective of the present work was to derive three alternative
98 parameterizations scenarios of the relationships between the CDOM absorption coefficient in
99 the Baltic and Pomeranian lakes waters and physical or biogeochemical variables. We have
100 performed analyses using combined data set of optical properties of marine and lacustrine
101 water samples, treating the data as a single, pooled set. Optical properties of lacustrine waters
102 displayed a resemblance to marine waters in the Baltic Sea, despite observed differences in
103 trophic status of those water bodies. According to Choiński (2007), lakes waters were divided
104 into ultraoligotrophic, oligotrophic, mesotrophic, eutrophic, hiperetrophic and dystrophic. The
105 trophicity is determines by the concentration of chlorophyll *a*, water transparency determined
106 by Secchi disk, and the concentration of biogenic factors, e.g. nitrogen and phosphorus
107 (Carlson, 1977; Kratzer and Brezonik, 1981). The ranges of concentrations of chlorophyll and
108 nutrients defining trophicity are higher than in marine waters. In our modelling approach we
109 have assumed that lakes could be treated as a natural extension of coastal, lagoon and river
110 mouth waters. The motivation for development of these models was to estimate a complete
111 spectrum of the CDOM light absorption coefficients by using different input parameters: *i*) in
112 the first scenario the known chlorophyll *a* concentration, *ii*) in the second scenario known
113 value of the CDOM absorption coefficient at 400 nm, $a_{\text{CDOM}(400)}$, *iii*) and in the third
114 scenario known value of $a_{\text{CDOM}(400)}$ and known nonlinear relationship between CDOM
115 absorption coefficient and the spectral slope coefficient *S*. Developed models can be used to
116 improve the accuracy of ocean colour remotes sensing algorithms for retrieval of
117 environmental variables in the Baltic Sea, adjacent estuaries and lagoons and fresh water
118 lakes.

119 **2. Material and methods**

120 *2.1 Sampling area*

121 Water samples for determination of optically significant water constituents
122 concentrations were collected from August 2006 to November 2009 in the southern Baltic and
123 in three lakes in the Pomeranian Lake District (Poland) during the long term observation
124 program of inherent and apparent optical properties for calibration and validation of ocean
125 colour satellite imagery products conducted by the Institute of Oceanology, Polish Academy
126 of Sciences, Sopot, Poland, (IOPAN). Location of 116 measuring stations, where empirical
127 data were gathered (a total of 413 data sets) during 16 cruises of *r/v Oceania* on the Baltic
128 were shown on Figure 1, and cruises details is given in the Table 1. Research cruises were



129 organized to capture the dynamics of natural seasonal variability occurring in temperate
130 waters: *i*) at the end of the winter before the onset of the spring phytoplankton bloom, when
131 wind-driven mixing, the vertical convective thermohaline circulation, reduced biological
132 activity and reduced riverine outflow all result in clearer surface waters; *ii*) in spring when the
133 spring phytoplankton bloom coincides with maximum freshwater runoff from Baltic Sea
134 watershed; *iii*) and at the end of summer at the peak of secondary phytoplankton blooms and
135 the period of maximal thermal stratification of waters. The geographical coverage of the
136 samples included the Gulf of Gdańsk, the Pomeranian Bay, the Szczecin Lagoon, Polish
137 coastal waters and the open sea (the Baltic Proper). The coastal sites in the Gulf of Gdańsk
138 and the Pomeranian Bay are under the direct influence of two major river systems, the Vistula
139 and the Odra, which drain the majority of Poland. Additionally samples were collected twice
140 a month on sampling station at the Sopot pier (Gulf of Gdańsk), from which 66 sets of data
141 were obtained. Field observation were also carried from April 2006 to November 2009 on
142 monthly intervals a month (except months when the surface of the lake was covered with ice)
143 in three Pomeranian lakes (Łebsko, Chotkowskie and Obłęskie) from which 77 data sets were
144 obtained. Selected lakes are closed water bodies with only small rivers flowing in and out of
145 them. Lake Łebsko is a specific case: it is a coastal lake and connected directly to the sea by a
146 short canal. Part of Lake Łebsko area immediately adjacent to the canal can, on occasion, be
147 inundated when large backflows of sea water enter the lake. The lake's water level can then
148 rise by 50-60 cm (Chlost and Cieśliński, 2005). Such a situation obviously affects the
149 composition and properties of the lacustrine water. Similar effects, resulting from the great
150 variability of water properties, can be expected at the points where rivers flow into lakes. The
151 lacustrine water in these areas is thus modified by the river water.

152 *2.2 Samples processing*

153 Discrete samples of water were taken from the surface layer of the southern Baltic and
154 the three Pomeranian lakes with use of the Niskin bottle. The samples for spectroscopic
155 measurements CDOM light absorption underwent a two-step filtration process. The first
156 filtration was through acid-washed Whatman glass fibre filters (GF/F, nominal pore size 0.7
157 μm). The water was then passed through acid washed Sartorius 0.2 μm pore cellulose
158 membrane filters to remove fine-sized particles. Spectrophotometric scans of CDOM
159 absorption spectra were performed with use the Unicam UV4-100 double beam
160 spectrophotometer installed both in land base laboratory and on board of the research ship in
161 the 240-700 nm spectral range. The cuvette pathlength was 5 cm and the MilliQ water was



162 used as the reference for all measurements. The absorption coefficient $a_{CDOM}(\lambda)$ was
 163 calculated using the following equation:

$$164 \quad a_{CDOM}(\lambda) = 2.303 \cdot A(\lambda) / L, \quad (2)$$

165 where: $A(\lambda)$, is the optical density, L is the optical path length in meters and the factor 2.303
 166 is the natural logarithm of 10.

167 A nonlinear least squares fitting method using a Trust-Region algorithm implemented
 168 in Matlab R2009 was applied (Stedmon et al., 2000, Kowalczyk et al., 2006) to calculate
 169 CDOM absorption spectrum slope coefficient, S , in the spectral range 300-600 nm using the
 170 following equation:

$$171 \quad a_{CDOM}(\lambda) = a_{CDOM}(\lambda_0) e^{-S(\lambda_0 - \lambda)} + K \quad (3)$$

172 where: λ_0 is 350 nm, and K is a background constant that allows for any baseline shift caused
 173 by residual scattering by fine size particle fractions, micro-air bubbles or colloidal material
 174 present in the sample, refractive index differences between sample and the reference, or
 175 attenuation not due to CDOM. The parameters $a_{CDOM}(350)$, S , and K were estimated
 176 simultaneously via non-linear regression using Equation 3.

177 The chlorophyll a concentration was determined with use pigment extraction method.
 178 Pigments contained within suspended particles were collected by filtration of water samples
 179 onto 47-mm Whatman glass-fiber filters (GF/F) under low vacuum and extracted 24 hours in
 180 96% ethanol at room temperature. Chlorophyll a , $Chla$, concentration was determined
 181 spectrophotometrically with a UV4-100 spectrophotometer (Unicam, Ltd). In this method the
 182 optical density (absorbance) of pigment extract in ethanol was measured at 665 nm. After
 183 correction for background signal in the near infrared (750 nm): $\Delta OD = OD(665\text{nm}) -$
 184 $OD(750\text{nm})$, the absorbance was converted to chlorophyll a concentration, using an equation
 185 involving the volumes of filtered water (V_w) [dm^3], and ethanol extract (V_{EtOH}) [cm^3], a 2-cm
 186 path length of cuvette (l), and the chlorophyll a specific absorption coefficient in 96% ethanol
 187 [$\text{dm}^3 (\text{g cm}^{-1})$] [Strickland and Parsons 1972; Stramska et al., 2003]:

$$188 \quad Chla = (10^3 \cdot \Delta OD \cdot V_{EtOH}) / (83 \cdot V_w \cdot l)^{-1}. \quad (4)$$

189 During field surveys temperature and salinity profiles were measured with and
 190 SeaBird SB36 CTD probe to provide background physical conditions during sampling.



191 The collected data were analyzed by the use of statistical package and data
 192 visualization software (SigmaPlot 8.1). Dynamic range of variability of analyzed optical
 193 parameters values exceeded 3 orders of magnitude, therefore logarithmic transformation was
 194 applied which allowed better presentation of their dynamics changes and to analyze
 195 statistically collected data set accordingly. Following arithmetic and logarithmic statistical
 196 metrics were used to assess uncertainty of developed empirical relationships and models:

197 • relative mean error (systematic): $\langle \varepsilon \rangle = N^{-1} \sum_i \varepsilon_i$ (where $\varepsilon_i = (X_{i,C} - X_{i,M}) / X_{i,M}$); (5a)

198 • standard deviation (statistical error) of ε (RMSE – root mean square error):

199
$$\sigma_\varepsilon = \sqrt{\frac{1}{N} \left(\sum (\varepsilon_i - \langle \varepsilon \rangle)^2 \right)}$$
 (5b)

200 • mean logarithmic error: $\langle \varepsilon \rangle_g = 10^{\left[\log(X_{i,C}/X_{i,M}) \right] - 1}$ (6)

201 • standard error factor: $x = 10^{\sigma_{\log}}$ (7)

202 • statistical logarithmic errors: $\sigma_+ = x - 1$ $\sigma_- = \frac{1}{x} - 1$ (8)

203 where $X_{i,M}$ - measured values; $X_{i,C}$ - estimated values (subscript M stands for 'measured';
 204 subscript C stands for 'calculated');

205 • $\langle \log(X_{i,C}/X_{i,M}) \rangle$ - mean of $\log(X_{i,C}/X_{i,M})$;

206 • σ_{\log} - standard deviation of the set $\log(X_{i,C}/X_{i,M})$.

207 3. Results

208 3.1 Variability of analysed parameters and empirical relationship between CDOM absorption 209 and spectral slope coefficient.

210 Variability range and average values of selected optical parameters: the light absorption
 211 coefficients by CDOM at two wavelengths: 375 and 400 nm; $a_{\text{CDOM}(375)}$ and $a_{\text{CDOM}(400)}$;
 212 spectral slope S , and chlorophyll a concentrations, $Chla$, measured in the study area and used
 213 for formulation of empirical model have been presented in the Table 2. The minima in of the
 214 variability ranges of $a_{\text{CDOM}(375)}$, $a_{\text{CDOM}(400)}$ and $Chla$, were noted in marine waters. The
 215 minimal values of CDOM absorption coefficients in lacustrine waters were almost an order of



216 magnitude higher than in marine waters, indicating significant accumulation of CDOM in
 217 fresh waters. The maximal values of $a_{\text{CDOM}(375)}$, $a_{\text{CDOM}(400)}$ and $Chla$ were observed in
 218 fresh waters, maximal values were approximately two time higher than values of respective
 219 parameters in marine waters. Consequently average values of the CDOM absorption
 220 coefficients: $a_{\text{CDOM}(375)}$, $a_{\text{CDOM}(400)}$, chlorophyll a concentration were higher in fresh waters
 221 compared to marine waters. The reverse trend is observed CDOM absorption spectrum slope
 222 coefficient, S , variability range: both of minimal and maximal spectral slope values were
 223 lower in the lakes than those observed in the marine waters. The average value of the spectral
 224 slope coefficient was higher in marine waters than in lake waters. These two data sets,
 225 measured in the Baltic waters and Pomeranian lakes were statistically significantly different,
 226 as indicated by results of simple analysis of variance: ($p = 3.4 \cdot 10^{-38}$). However, their
 227 variability ranges were such that the data from the two different aquatic environments were
 228 overlapping creating coherent data set, that could be analysed together. Our principle
 229 assumption for the derivation of CDOM absorption model was that, the optical properties of
 230 lacustrine waters could be treated as they were an extension of estuarine and marine waters.

231 The spectral slope coefficient was inversely non-linearly related with the CDOM
 232 absorption coefficient. The highly absorbing samples were spectrally flatter (characterised by
 233 lower S value). Different functional types were used to model this relationships: hyperbolic
 234 (Stedmon and Markager, 2001, Kowalczyk et al., 2006), or logarithmic (Kowalczyk et al.,
 235 2005). For consistency with Kowalczyk (2001) we have used the log-linear fit to describe the
 236 relationship between $a_{\text{CDOM}(400)}$ and S . The distribution of the spectral slope in the function
 237 of CDOM absorption coefficient in the Baltic Sea (black dots) and Pomeranian lakes (green
 238 dots) has been presented on the Figure 2a. The black line presents log-linear dependence
 239 (Equation 9), obtained by Kowalczyk (2001), overlaid on our data set:

$$240 \quad S = \log[1.038 a_{\text{CDOM}(400)}^{-0.022}]. \quad (9)$$

241 The old relationship worked satisfactory for part of Baltic Sea data set ($R^2 = 0.76$), but
 242 it does not cover large group of CDOM absorption coefficients values larger than 5 m^{-1} . The
 243 $a_{\text{CDOM}(400)} > 5 \text{ m}^{-1}$ were measured in the lakes and in estuarine waters and in the Szczecin
 244 Lagoon and Vistula and Odra mouth inflowing into southern Baltic. We have derived a new
 245 formulae to determine the $a_{\text{CDOM}(400)}/S$ relationship that covered whole range of the
 246 $a_{\text{CDOM}(400)}$ observed both the Baltic Sea and in Pomeranian lakes waters. The new formulae
 247 was marked on Figure 2.a as red curve and is described by Equation 10.



248
$$S = 0.0213 - 0.003 \ln[a_{CDOM}(400)]. \quad (10)$$

249 The new $a_{CDOM}(400)/S$ relationship has been found much better constrained and explained
250 much more variance ($R^2 = 0.79$) with less uncertainty (RMSE = 0. 1%) compared to one
251 presented by Kowalczuk (2001).

252 Detailed analysis of distribution of spectral slope in the function of $a_{CDOM}(400)$
253 indicated that data set could be divided in respect to salinity, into two subsets: samples
254 characterised by salinity above 5 (mostly Baltic Sea water samples) and those with salinity
255 below 5, which include waters from river mouths, lakes and the Szczecin Lagoon. The
256 relationship between $a_{CDOM}(400)$ and S derived for respective data subsets were presented on
257 Figure 2.b and functional formulae were given by Equation 11 (salinity > 5) and Equation 12
258 (salinity < 5)

259
$$S = 0.0206 - 0.004 \ln[a_{CDOM}(400)] \quad (11)$$

260
$$S = 0.0196 - 0.0009 \ln[a_{CDOM}(400)]. \quad (12)$$

261 Proposed approximations of $a_{CDOM}(400)/S$ relationships in two salinity ranges were
262 characterised by the higher explained variance ($R^2 = 0.78$ for Equation 11, and lower
263 $R^2 = 0.22$, for Equation 12, respectively. In both cases, the estimation uncertainty:
264 RSME = 0.08% for Equation 11, RSME = 0.09%, for Equation 12, respectively, were lower
265 compared to approximation presented by Equation 10.

266 *3.2. A model for approximation of CDOM light absorption spectrum from empirical*
267 *dependency with the chlorophyll a concentration.*

268 The principle bio-optical assumption on interdependencies among optically significant
269 water constituents in global ocean was formulated by Morel and Prieur (1977), who
270 introduced the concept of the Case 1 water, where variability of those constituents is to far
271 extent correlated with variability of phytoplankton biomass expressed as chlorophyll *a*
272 concentration. The Case 1 waters were mostly open oceanic waters and upwelling region at
273 western continental margins. The marine basins where these assumption were not fulfilled
274 were considered Case 2 water: mostly semi-enclosed and shelf seas and coastal ocean, where
275 there were sources of riverine waters. It was assumed that changes in magnitude of optically
276 significant water constituents in the Case 2 waters were independent. This concept was
277 critically reassessed by Siegel et al. (2005) who reanalyzed the global ocean colour imagery



278 data set and proved that, although in open ocean the bio-optical assumption is still valid, there
 279 were significant dependences between chlorophyll *a* and other optically significant water
 280 constituents at regional scales in oceanic continental margins. Even though the CDOM was
 281 not thought to be correlated with chlorophyll *a* concentrations in Case 2 waters, there were
 282 examples showing that such a relationships were possible (Ferrari and Tassan, 1992; Vodacek
 283 et al., 1997). In the Baltic waters such analyses were carried out by Kowalczyk and
 284 Kaczmarek (1996) and Kowalczyk (1999). These authors demonstrated that the correlation
 285 between the concentration of chlorophyll *a* and the CDOM absorption coefficient was
 286 observed. The positive correlation between light absorption by CDOM chlorophyll *a*
 287 concentration has been confirmed with new data available, both in marine and fresh waters.
 288 The clear trend of increase of CDOM absorption level with increasing phytoplankton biomass
 289 has been presented on Figure 3. The dependence between $a_{CDOM}(400)$ coefficient and the
 290 concentration *Chla* obtained by Kowalczyk (2001) has been overlaid on the new, currently
 291 reported empirical data set, Figure 3. It is evident that $a_{CDOM}(400)/Chla$ relationship reported
 292 by Kowalczyk's is applicable to only some of the Baltic Sea data, in chlorophyll *a*
 293 concentration range $0.8 < Chla < 10 \text{ mg m}^{-3}$. The old, power function relationship did not
 294 reproduced correctly the $a_{CDOM}(400)$ values for high chlorophyll *a* concentration, and CDOM
 295 absorption data measured in estuaries and lakes were lying above the model curve. We have
 296 proposed new statistically significant relationship between the $a_{CDOM}(400)$ and *Chla* which
 297 was described by a second-degree polynomial ($R^2 = 0.83$, RMSE = 28%, $n = 541$, $p < 0.0001$).

298 The same function has been applied to reconstruct the complete CDOM absorption
 299 spectrum in the spectral range from 245 to 700 nm with 5 nm resolution, Equation 13:

$$300 \quad a_{CDOM}(\lambda) = 10^{(A(\lambda)\log Chla)^2 + B(\lambda)\log Chla + D(\lambda)}, \quad (13)$$

301 where $A(\lambda)$ [$\text{m}^5 \text{mg}^{-2}$], $B(\lambda)$ [$\text{m}^2 \text{mg}^{-1}$], $D(\lambda)$ [m^{-1}] are the regression coefficients.

302 The spectral distribution of the regression coefficients and determination coefficient
 303 have been presented on Figure 4 and their values were included in Table A in Appendix A.
 304 Both regression coefficients $A(\lambda)$ and $B(\lambda)$ showed relatively small spectral variation in the
 305 UV and part of the visible spectral range. The biggest changes in regression coefficients
 306 spectra have been noted above 580 nm, where significant increase of the $A(\lambda)$ has been
 307 relatively compensated with decrease of the $B(\lambda)$. Spectral distribution of regression
 308 coefficient A , indicated a potential influence of the phytoplankton pigments absorption on the
 309 CDOM absorption spectrum as its maximum situated around 675 nm, overlaps with long



310 wave maximum of chlorophyll *a* absorption spectrum. This effect is visible only at longer
311 wavelength because the principle chlorophyll *a* maximum at 440 nm, is masked by CDOM
312 absorption especially at very turbid estuarine and fresh water, where highest values of CDOM
313 absorption were recorded. Free term $D(\lambda)$ spectrum decreases monotonically with increased
314 wavelength resembles the of the log transformed CDOM absorption coefficient spectrum
315 corresponding to the average CDOM absorption spectrum at a chlorophyll *a* concentration of
316 1 mg m^{-3} as shown on Figur 4.c. The spectral distribution of the determination coefficient
317 values R^2 , presented on Figure 4.d, demonstrated that, the model based on the dependency
318 between CDOM absorption coefficient and chlorophyll *a* concentration, explained more than
319 80% variability in $a_{\text{CDOM}}(\lambda)$ in UV and VIS, and this variability was controlled by
320 phytoplankton biomass production. The model performance deteriorated at wavelength longer
321 than 550 nm.

322 The model uncertainty has been passed and uncertainty analysis result for selected
323 wavelengths have been summarized in Table 3 and presented on Figure 5. Comparison
324 between estimated vs. measured $a_{\text{CDOM}}(\lambda)$ values at selected wavelengths (260, 350, 440,
325 500, 550, 600 nm) from range 240 – 700 nm were shown on first six upper panels Figure 5 (a-
326 f). Histograms of ratio between estimated and measured values at the same wavelength were
327 presented on lower six Figure 5 panels (g-l). The deterioration of model performance with
328 increasing wavelength has been evident. The overall uncertainty expressed by arithmetic
329 statistics and logarithmic statistics is satisfactory up to 500 nm, and then both systematic and
330 statistical estimation errors increased rapidly at longer wavelength. The arithmetic systematic
331 error has increased from 1.47% at 260 nm to 19.54% at 600 nm, arithmetic statistical error has
332 increased from 17.03% at 260 nm, to 79.13% at 600 nm respectively. Logarithmic uncertainty
333 metrics indicated that, standard error factor estimated for the entire spectral range from 240 to
334 700 nm of light absorption coefficients varies from 1.19 to 2.66. This means that the statistical
335 logarithmic error varies from -62% to +165%. The logarithmic systematic errors in the all 240
336 - 700 nm range do not exceed 3%.

337 *3.3. An empirical model for approximation of CDOM light absorption spectrum based on*
338 *empirical dependency with the CDOM absorption coefficient value at 400 nm, $a_{\text{CDOM}}(400)$.*

339 The exponential model for CDOM absorption requires information on two input
340 parameters: magnitude of CDOM absorption at reference wavelength and spectral slope
341 value. However, the monotonic property of CDOM absorption spectrum determines the high



342 level of interdependency of absorption coefficient values across considered spectral range and
 343 allows omit the detailed information on spectral slope. The second model that we have
 344 developed is based on the dependence of light absorption by CDOM at any given wavelength
 345 and the CDOM absorption coefficient at wavelength 400 nm. Many authors treat this
 346 wavelength as a reference for CDOM absorption using the exponential Equation 1 (e.g.
 347 Kowalczyk et al., 2005; Woźniak and Dera, 2007). It was also recommended by
 348 Sathyendranath et al. (1989) to distinguishing between dissolved organic matter absorption
 349 from that caused by phytoplankton. In optically complex waters (Baltic Sea and the lakes),
 350 $a_{CDOM}(400)$ makes up the large proportion of the total absorption of light in water,
 351 (Kowalczyk, 2001; Ficek 2013).

352 The interdependency of spectral CDOM absorption values has been assessed by
 353 Kowalczyk (2001) who analysed the linear cross-correlation matrix between $a_{CDOM}(\lambda)$ values
 354 measured at different wavelengths. The linear interrelationship between $a_{CDOM}(\lambda)$
 355 deteriorated with increasing spectral distance from reference wavelength both toward shorter
 356 and longer wavelengths. To better reflect the non-linear property of CDOM absorption
 357 spectrum we have used the second order polynomial model based on log transformed
 358 $a_{CDOM}(\lambda)$ values as input variable. Calculation were performed in the spectral range 240 –
 359 700 nm, with 5 nm resolution. The statistical analyses yielded the formula:

$$360 \quad a_{CDOM}(\lambda) = 10^{(M(\lambda)\log(a_{CDOM}(400))^2 + N(\lambda)\log(a_{CDOM}(400)) + O(\lambda))}, \quad (14)$$

361 where $M(\lambda)$ [m], $N(\lambda)$ [dimensionless] and $O(\lambda)$ [m^{-1}] are the parameterization coefficients
 362 shown graphically in Figure 6. Their values for the 240 – 700 nm range are listed in Table B
 363 (in Appendix A).

364 The spectral shape of the regression coefficients $M(\lambda)$, $N(\lambda)$ and free term $O(\lambda)$ that
 365 were derived for empirical model that used the $a_{CDOM}(400)$ value as independent variable,
 366 were quite similar to spectral shape of regression coefficient and free term of the model based
 367 on chlorophyll *a* concentration. The regression $M(\lambda)$, and $N(\lambda)$ were also characterised by
 368 maxima located in the red part of the light spectrum. Similarly to the first presented model,
 369 the spectral shape of the free term $O(\lambda)$ resembled the log-transformed CDOM absorption
 370 spectrum. The spectral distribution of the determination coefficient R^2 indicated that
 371 approximation of $a_{CDOM}(\lambda)$ values based on the magnitude of the CDOM absorption at



372 reference wavelength was much more accurate than approximation based on chlorophyll *a*
373 concentration. The R^2 values were over 0.9 in ultraviolet part of the spectrum approaching 1,
374 near the reference value, and fell down below 0.8 at 560 nm.

375 The second model uncertainty has been passed, and uncertainty analysis result for the
376 same wavelengths as previously used, have been summarized at Table 4 and presented on
377 Figure 7 as presented in Table 3. Comparison between estimated vs. measured $a_{CDOM}(\lambda)$
378 values at six selected wavelengths were shown on first six upper panels Figure 7 (a-f).
379 Histograms of ratio between estimated and measured values at the same wavelength were
380 presented on lower six Figure 7 panels (g-l). The deterioration of model performance with
381 increasing wavelength has been much smaller than in case of CDOM absorption spectrum
382 approximation based on the chlorophyll *a* concentration. The overall uncertainty expressed by
383 arithmetic statistics and logarithmic statistics was much better up to 550 nm. Similarly, to the
384 first model both systematic and statistical estimation errors increased at longer wavelength.
385 The arithmetic systematic error has increased from 0.38% at 260 nm to 16.64% at 600 nm,
386 arithmetic statistical error has increased from 9.11% at 260 nm, to 67.45% at 600 nm
387 respectively. Logarithmic uncertainty metrics indicated that, standard error factor estimated
388 for the entire spectral range from 240 to 700 nm of light absorption coefficients varies from
389 1.09 to 1.76. This means that the statistical logarithmic error varies from -43% to +75%. The
390 systematic errors in the 240 - 700 nm interval did not exceed 2%

391 *3.4 Two-parametrical model for estimating of CDOM absorption in the Baltic Sea and* 392 *Pomeranian Lakes*

393 Earlier we showed two alternative one-parameter models of CDOM absorption which
394 estimating values of $a_{CDOM}(\lambda)$ at different wavelengths with relatively low errors. However,
395 there is a two-parameter model, developed by Kowalczyk et al. (2006) for the Baltic Sea
396 waters, which we decided to analyze in this study data for comparison. This statistical model
397 for estimation of CDOM absorption coefficient at 375 nm, $a_{CDOM}(375)$ at surface waters was
398 based on the seasons and the chlorophyll *a* concentration that acted as a proxy for
399 autochthonous production of CDOM. We have used the non-linear relationship between the
400 CDOM absorption coefficient $a_{CDOM}(375)$ and spectral slope to derive *S*, and used it later for
401 CDOM absorption spectrum reconstruction using classical exponential model (Equation 1).



402 The dependence between slope S and $a_{\text{CDOM}(375)}$ coefficient obtained by Kowalczuk et al.
403 (2006) has been overlaid on the currently reported empirical data set, Figure 8. The
404 $S/a_{\text{CDOM}(375)}$ relationship reported by Kowalczuk et al., (2006) is applicable to most of the
405 Baltic Sea and lakes data in within the $a_{\text{CDOM}(375)}$ range $1.5 - 14.16 \text{ m}^{-1}$ (mainly estuaries
406 and lakes waters). That hyperbolic relationship did not reproduced correctly the S values for
407 $a_{\text{CDOM}(375)}$ values below 1.5 m^{-1} , and slopes measured in open and mostly coastal Baltic
408 waters were lying below the model curve. We have proposed similar hyperbolic statistically
409 significant relationship between the S and $a_{\text{CDOM}(375)}$ which could better fit to current data
410 set. The determination coefficient of update hyperbolic function was very high: $R^2 = 0.86$,
411 $\text{RMSE} = 0.08\%$, $n = 541$, $p < 0.0001$. The new empirical relationship between spectral slope S ,
412 and $a_{\text{CDOM}(375)}$ is given by formula (15):

$$413 \quad S = 0.01722 + \frac{0.0057}{0.0407 + a_{\text{CDOM}(375)}} \quad (15)$$

414 The new formulae was applied Equation 1 to calculate the CDOM absorption
415 spectrum in the spectral range between 240 - 700 nm. The uncertainty of the exponential
416 model that used the spectral slope variable estimated from the new approximation given by
417 Equation 15 have been assed and uncertainty analysis result for selected wavelengths have
418 been summarize at Table 5. For comparison we have also done uncertainty analysis of the
419 exponential model with spectral slope variable estimated from the S and $a_{\text{CDOM}(375)}$
420 relationships presented by Kowalczuk et al. (2006). The uncertainty analysis has revealed that
421 two parameter estimation of the CDOM absorption spectrum was less accurate that two first
422 one parameters models. The spectral values of CDOM absorption estimated form the
423 exponential relationship and spectral slope parameterization with use of Kowalczuk et al.
424 (2006) and current empirical formulas were systematically overestimated in UV and
425 underestimated in visible spectral range. The systematic and statistical errors were increasing
426 toward the red part of the spectrum. The highest uncertainty, that exceeded 30% in systematic
427 error and 20% in statistical error were noted at wavelengths longer than 500 nm. Use of
428 current empirical spectral slope parameterization enables estimation of spectral $a_{\text{CDOM}(\lambda)}$
429 values with relatively lower errors, compared to results given by the same approach with use
430 of Kowalczuk et al. (2006) slope parameterization.

431



432 4. Discussion

433 Presented dataset part of the above 25 timer series of bio-optical data collected in
434 IOPAN in the Baltic Sea. This subset was created to match the observations conducted in the
435 2006 - 2009 in Pomeranian lakes by Ficek et al., (2012) and Ficek (2013) and enabled
436 extended analysis on data characterized by large dynamic variability range that in some cases
437 exceeded three orders of magnitude. Seawaters and lake waters were analyzed as a single
438 database, despite some differences in the compositions of optically active components of
439 these waters, treating the lakes as a natural extension of marine waters with properties
440 resembling the properties of estuaries. Coefficients of $a_{CDOM}(\lambda)$ in analyzed waters varies in 3
441 orders of magnitude (for example $a_{CDOM}(375)$ varies from 0.41 to 14.16 m^{-1} , $a_{CDOM}(400)$
442 varies from 0.15 to 8.85 m^{-1}). Spectral slope $S_{300-600}$ in Baltic and lakes varies in range 0.007 –
443 0.03 nm^{-1} , while the *Chla* concentration varied in range up to 3 orders of magnitude from 0.72
444 to 119 $mg\ m^{-3}$. Ranges of variability of parameters analyzed in this paper corresponded with
445 the data presented in earlier work on the optical properties in the Baltic Sea (Babin et al. 2003,
446 Kowalczyk 1999, Kowalczyk et al. 2005, 2006, 2010) or Pomeranian lakes (Ficek et al. 2012;
447 Ficek 2013). Ficek (2013) reported that in Pomeranian lakes *Chla* concentrations can may be
448 even 336 $mg\ m^{-3}$.

449 In this paper we have presented two single-parameter models and one two-parameter
450 model, which we use for calculation spectral values CDOM absorption coefficients $a_{CDOM}(\lambda)$
451 in a broad spectral range in Baltic Sea waters and the Pomeranian lakes. First two models
452 based on one single independent variable were characterized by similar uncertainty level,
453 which was in order of 1.5 - 7% in UV and visible spectral range, when chlorophyll *a* was used
454 as the independent variable or in order of 0.4 - 2.2 %, in the same spectral range when
455 $a_{CDOM}(400)$ was used as independent variable. For example, the statistical errors listed in
456 Table 3 for the parameterization dependent on the chlorophyll *a* concentration (13) and in
457 Table 4 for model (14) shows that the statistical arithmetic error is higher in the former case –
458 e.g. for 440 nm it is 4.01% – whereas in the latter case it is 0.42%. The second one parameter
459 model was characterized by lower uncertainty and higher spectral values of the determination
460 coefficient. Likewise, the standard error factor in the first model is higher than in the one
461 based on the dependence of the absorption $a_{CDOM}(\lambda)$.

462 The accuracy of both models have deteriorated at wavelength longer than 550 nm. One
463 possible explanation is the precision of the CDOM measurements. The use of 5 cm cuvettes



464 allowed the reliable CDOM absorption detection at $a_{CDOM}(\lambda)$ larger than 0.046 m^{-1} . The
465 spectrophotometer detection limit has been reached usually at wavelengths longer than 550
466 nm. Therefore the modeled values were usually compared to measured values that were
467 heavily impacted by errors resulted from measurements accuracy. One of the possible way of
468 increasing the spectrophotometric accuracy of CDOM absorption measurements would rely
469 on increasing cuvettes pathlength (maximum cuvettes pathlength used in most desktop
470 spectrophotometers would not exceed 10 cm), or use the optical waveguide
471 spectrophotometer systems that offer the optical pathlength in range of 0.2 meter to 2 meters
472 by (D'Sa et al., 1999; Miller et al. 2002). However usage of long measurements pathlength in
473 optically complex water such as Baltic Sea and fresh water lakes would severely impact the
474 radiometric sensitivity of any spectrophotometer, causing the fast decrease of light intensity
475 reaching the detector especially in the UV spectral range.

476 There were number of regional studies presenting the dependence between
477 chlorophyll *a* concentration, *Chla* and CDOM absorption $a_{CDOM}(\lambda)$, similar to our
478 parameterization described by Equation 13 (Ferrari and Tassan, 1992, Tassan 1994, Vodacek
479 et al. 1997, Morel et al. 2007, Morel and Gentili 2009, Bricaud et al. 2010, Organelli et al.
480 2014). We have compared the $a_{CDOM}(\lambda)/Chla$ relationship derived by us with selected
481 relationships between CDOM absorption coefficients $a_{CDOM}(\lambda)$ and *Chla* concentrations for
482 selected wavelengths developed by different authors for different water types. Selected model
483 outputs were overlaid on the observed distribution of $a_{CDOM}(\lambda)$ in the function of *Chla*,
484 presented on Figure 9. These relationships in all cases were approximated by power functions,
485 and assumed different rates of increase of the $a_{CDOM}(\lambda)$ value with increasing *Chla* (Tassan,
486 1994; Morel et al., 2007; Morel and Gentili 2009; Bricaud et al. 2010). Relationships
487 developed by other authors, were not suitable for estimating CDOM absorption in the Baltic
488 Sea waters and lakes. Empirical relationships developed by Tassan, (1994), Morel et al.,
489 (2007), Morel and Gentili (2009) and Bricaud et al. (2010) all underestimated the CDOM
490 absorption in Baltic Sea. Such a large mismatch between estimated and observed CDOM
491 absorption values certainly resulted from the fact that these relationships were developed for
492 clean oceanic waters where the contribution of dissolved organic material to the total light
493 absorption light was lower than in the Baltic Sea and the concentration of *Chla* did not exceed
494 40 mg m^{-3} . For example, Bricaud et al. (2010) have based their empirical model on
495 measurements from mesotrophic waters around the Marquesas Islands to hyperoligotrophic
496 waters in the subtropical gyre and eutrophic waters in the upwelling area west off Chilean



497 coast (South Pacific), where observed *Chla* concentrations spanned more than two orders of
498 magnitude (0.017 to 1.5 mg m^{-3}) in the surface layer; observed values of the spectral slope, S ,
499 contained within the range of 0.007 - 0.032 nm^{-1} ; and observed $a_{CDOM}(440)$ values were from
500 0.0003 to 0.038 m^{-1} . Morel et al. (2007) carried out measurements in hyperoligotrophic waters
501 in the South Pacific gyre (near Easter Island), where observed *Chla* concentrations were
502 within range of 0.022 to 0.032 mg m^{-3} in the surface layer. Tassan (1994) reported two
503 relationships between $a_{CDOM}(\lambda)$ and *Chla* (one for Gulf of Naples waters and second for
504 Adriatic Sea), and then used these relationships for estimation of CDOM absorption
505 coefficient values at different ranges of *Chla* concentrations (0.25 to 40 mg m^{-3}). Morel and
506 Gentili (2009) tested developed satellite ocean color algorithm enabling determination of the
507 CDOM absorption and the *Chla* concentration from satellite imagery in Mediterranean
508 waters, where *Chla* varied within the range from 0.01 to 0.5 mg m^{-3} . The eutrophic Baltic Sea
509 waters and superthrophic lakes water were characterized by high significantly higher *Chla*
510 concentrations. The total absorption in our study area were dominated by absorption organic
511 dissolved substances (Woźniak et al., 2011; Ficek et al., 2012), which has of both the
512 autochthonous and allochthonous origin, therefore observed spectral CDOM absorption
513 coefficient valued per unit of chlorophyll a concentrations were almost twice as much in the
514 Baltic Sea and Pomeranian lake than those observed in oceanic waters in the Pacific and
515 marine water in the Mediterranean and Adriatic. These findings underlined need for
516 development of regional algorithms and bio-optical models, because those developed in other
517 regions did not accounted the constant and very high background in CDOM absorption
518 persistently prevalent in the Baltic Sea and fresh water in temperate climatic zone.

519 The uncertainty analysis proved that, both mathematical one-parametrical CDOM
520 absorption estimations presented in this paper performed better, than classical exponential
521 model with variable slope non-linear parameterization by Kowalczyk et al. (2006) and its
522 modification presented in Equation 15. Comparison of tables 3, 4 and 5 showed, that in any
523 case, the estimation accuracy decreases with the wavelength, however the two parameters
524 exponential model significantly underestimated $a_{CDOM}(\lambda)$ at longer wavelengths. Standard
525 error factor x (indicating how many times approximated values were different from measured)
526 is lower in the Kowalczyk et al. (2006) model and our modification of this model than
527 approximations (13) and (14). But systematic errors, both arithmetic and logarithmic, are
528 much higher. For example in models by Kowalczyk et al. (2006) for the 440 nm wavelength
529 arithmetic systematic error takes average value -16% and logarithmic systematic error takes



530 average value -17%, while using the formula (13), we have 4% and 0.01%, and for the
531 formula (14) 0.4% and 0.003%, respectively. Morel and Gentili (2009) and Morel et al.
532 (2010) derived a two-component model for description of the CDOM absorption properties,
533 and they modelled the spectral slope values using its empirical relationship with the
534 chlorophyll *a* concentration. These models were based on data sets collected in clear oceanic
535 waters, so their applicability to Baltic Sea conditions would probably be questionable as it
536 was in case of the $a_{\text{CDOM}}(\lambda)/Chla$ relationships.

537 Finally, we have compared the performance in the retrieval of CDOM absorption spectrum in
538 the Baltic Sea conditions of two standard exponential models broadly used in optical
539 oceanography: *i*) model by Bricaud et al. (1981) with spectral slope $S_{375-500}$ and CDOM
540 absorption reference wavelength $\lambda_0 = 375$ nm, *ii*) model by Babin et al. (2003) with spectral
541 slope, $S_{350-500}$ and CDOM absorption reference wavelength $\lambda_0 = 443$ nm) and model
542 Kowalczyk et al. (2006). The modelled spectra were presented on Figure 10, together with
543 measured CDOM absorption spectra and those calculated from one-parameter models
544 expressed by Equations 13 and 14. Empirical model developed for Baltic Sea and inland
545 waters - Equations 13 and 14, based on locally observed variability in biogeochemical and
546 optical variables adequately reflected the real, spectrophotometrically measured light
547 absorption coefficients. The model based on the dependence of the chlorophyll *a*
548 concentration, Equations 13, best fits the coefficients for wavelengths from 240 to 600 nm,
549 and could applied in variety of water bodies with contrasting trophic status. From this point of
550 view, therefore, it is far superior to the models derived by Bricaud et al. (1981) or Babin et al.
551 (2003), which were developed either for oligotrophic or mesotrophic oceanic waters, or for
552 European coastal water but with incorporating bio-optical properties of fresh waters. On the
553 other hand model Kowalczyk et al. (2006) underestimates values of $a_{\text{CDOM}}(\lambda)$.

554 In order to compare the above-mentioned models, we adapted them to the empirical
555 data set presented in this study within the spectral range from 240 to 700 nm, and then we
556 have applied the same statistical metrics to assess their uncertainty. Calculated errors were
557 listed in Table 6 for selected wavelengths. The systematic errors in arithmetic statistics were
558 higher in selected error compared to one parameters models presented by us. The systematic
559 errors calculated for CDOM absorption model by Babin et al., (2003) were significantly
560 higher in all selected wavelengths compared to those presented in Tables 3 and 4. The CDOM
561 absorption could be estimated by empirical model based on the a the $a_{\text{CDOM}}(\lambda)/Chla$



562 dependency with the systematic error of 3.13 % at $\lambda = 350$ nm, whereas Babin et al., (2003)
563 model estimated the CDOM absorption at the same wavelength with systematic error of -
564 33.70%. Calculated statistical errors of the estimates with use of the Bricaud et al. (1981) and
565 Babin et al. (2003) models were very large compared to the results obtained with models
566 expressed by Equations 13 and 14. Whereas the standard error factors are quite good for
567 Bricaud's model (from 1 to 2.43), they are much higher for Babin's model (from 1.045 to
568 3.58). However, in both cases, the systematic errors are large: -59% to 144–and 79% to
569 +400%, respectively.

570 **5. Conclusion**

571 We have demonstrated that CDOM absorption was non-linearly correlated with
572 chlorophyll *a* concentration in broad variability range spanning over three orders of
573 magnitude in marine waters of the Baltic Sea, its estuaries, coastal lagoons and in the fresh
574 water lakes characterised by different trophic status. The second order polynomial
575 approximation the relationship between chlorophyll *a* concentration and $a_{\text{CDOM}(400)}$ could be
576 used to in both marine and fresh water, and was much more accurate than one derived for
577 Baltic Sea waters by Kowalczuk (2001). This relationship has also proved that optical and
578 bio-optical properties of marine and fresh waters could be regards as an continuum in regard
579 of CDOM absorption and chlorophyll *a* concentration. We have had derived models for
580 estimation of CDOM light absorption by spectrum in the spectral range 240-700 nm from
581 chlorophyll *a* concentrations *Chla* or from coefficients of light absorption by CDOM for
582 wavelength 400 nm ($a_{\text{CDOM}(400)}$). For comparison we have also, tested the classical
583 exponential model for approximation CDOM absorption spectrum, where the spectral slope
584 coefficient was determined from nonlinear relationship between spectral slope coefficient and
585 values of $a_{\text{CDOM}(375)}$. The uncertainty analysis results proved that, the one-parametric,
586 second order polynomial function of the chlorophyll *a* concentration, *Chla*, enabled
587 estimation of spectral values of CDOM absorption coefficient, $a_{\text{CDOM}(\lambda)}$ with slightly lower
588 accuracy than, its estimation based on second order polynomial function of the CDOM
589 absorption coefficient at wavelength 400 nm $a_{\text{CDOM}(400)}$. Presented models, optimized for
590 Baltic Sea and fresh water specific optical and bio-optical conditions, were characterized with
591 significantly lower errors of estimations compared to widely used CDOM absorption model
592 proposed by other authors. The CDOM absorption models presented in this study, could be
593 used for improvements of remote sensing algorithms designed for retrievals of various optical



594 and bio-optical parameters needed for characterization and monitoring of the state and
595 functioning of the Baltic Sea and Pomeranian lakes ecosystems. Validation of these models
596 showed that they can be reliably applied in monitoring surveys, when a rapid, approximation
597 the light absorption spectrum is needed.

598 **Acknowledgements**

599 This paper was prepared as a part of project N N306 041136 financed by the Polish Ministry
600 of Science and Higher Education in 2009-2014 and also within the framework of the
601 SatBałtyk project funded by the European Union through the European Regional
602 Development Fund, (No. POIG.01.01.02-22-011/09, 'The Satellite Monitoring of the Baltic
603 Sea Environment'). The Institute of Oceanology, Polish Academy of Sciences provided the
604 funds for part of this study within the framework of the Statutory Research Project.

605 **References**

- 606 1. Arrigo K., Brown Ch., 1996. Impact of chromophoric dissolved organic matter on UV
607 inhibition of primary productivity in the sea. *Mar. Ecol. Prog. Ser.*, 140, 207-216.
- 608 2. Babin M., Stramski D., Ferrari G. M., Claustre H., Bricaud A., Obolensky G.,
609 Hoepffner N., 2003. Variations in the light absorption coefficient of phytoplankton,
610 nonalgal particles, and dissolved organic matter in coastal waters around Europe, *J.*
611 *Geophys. Res.*, 108(C8), 3211.
- 612 3. Bricaud A., Morel A., Prieur L., 1981. Absorption by dissolved organic matter of the
613 sea (yellow substance) in the UV and visible domains, *Limnol. Oceanogr.*, 26: 43-53.
- 614 4. Bricaud, A., M. Babin, H. Claustre, J. Ras, and S. Tièche. 2010. Light absorption
615 properties and absorption budget of Southeast Pacific waters, *J. Geophys. Res.*
616 115:C08009, doi:10.1029/2009JC005517.
- 617 5. Campanelli A., Bulatovic A., Cabrini M., Grilli F., Kljajić Z., Mosetti R., Paschini E.,
618 Penna P., Marini M., 2009. Spatial distribution of physical, chemical and biological
619 oceanographic properties, phytoplankton, nutrients and Coloured Dissolved Organic
620 Matter (CDOM) on the Boka Kotorska Bay (Adriatic Sea). *Geofizika*, 26(2), 215-228.
- 621 6. Carlson R. E., 1977. A trophic state index for lakes, *Limnol. Oceanogr.*, 22, 361-369.
- 622 7. Chlost I., Cieśliński R., 2005. Change of level of waters Lake Łebsko, *Limnol. Rev.* 5,
623 17-26.
- 624 8. Choiński A., 2007. Physical limnology of Poland, Eds. UAM, Poznań, 547, (in polish).



- 625 9. D'Sa, E.J., Steward, R.G., Vodacek, A., Blough, N.V., Phinney, D., 1999. Determining
626 optical absorption of colored dissolved organic matter in seawater with a liquid
627 capillary waveguide. *Limnol. Oceanogr.* 44, 1142–1148.
- 628 10. Darecki M. and D. Stramski, 2004. An evaluation of MODIS and SeaWiFS bio-optical
629 algorithms in the Baltic Sea. *Remote Sens. Environ.*, 89(3), pp. 326-350.
- 630 11. Darecki, M., A. Weeks, S. Sagan, P. Kowalczyk, and S. Kaczmarek. 2003. Optical
631 characteristics of two contrasting case 2 waters and their influence on remote sensing
632 algorithms. *Cont. Shelf Res.* 23(3-4):237-250.
- 633 12. Ferrari G. M., Tassan S., 1992. Evaluation of the influence of yellow substance
634 absorption on the remote sensing of water quality in the Gulf of Naples: a case study,
635 *Int. J. Remote Sens.*, 13(12), 2177-2189.
- 636 13. Ficek D., 2013, Bio-optical properties of lakes in Pomerania and their comparison
637 with the properties of other lakes and Baltic Sea waters, *Dissertations and Monographs*
638 *IO PAS 23/2013*, Institute of Oceanology Polish Academy of Sciences (in polish),
639 pp351.
- 640 14. Ficek D., T. Zapadka, J. Dera, 2011. Remote sensing reflectance of Pomeranian lakes
641 and the Baltic, *Oceanologia* 53(4):959-970.
- 642 15. Ficek D., Meler J., Zapadka T., Woźniak B., Dera J., 2012. Inherent optical properties
643 and remote sensing reflectance of Pomeranian lakes (Poland), *Oceanologia*, 54(4),
644 611-630.
- 645 16. Górniak A., 1996, Humic substances and their role in the functioning of freshwater
646 ecosystems, Warsaw University, Białystok Branch, 151 (in polish).
- 647 17. Jerlov, N.G., 1976. *Marine Optics*. Elsevier, New York (231 pp.).
- 648 18. Kieber D.J., Peake B.M., Scully N.M., 2003. Reactive oxygen species in aquatic
649 ecosystems, [in:] *UV effects in aquatic Organisms*, Helbling E.W., Zagarese H. (ed.),
650 Royal Society of Chemistry, Cambridge, UK, 251–288.
- 651 19. Kirk J. T. O., 1994. *Light and Photosynthesis in Aquatic Ecosystems*, Cambridge
652 University Press, London-New York, 509.
- 653 20. Kowalczyk P., 1999. Seasonal variability of yellow substances absorption in the
654 surface layer of the Balic Sea, *J. Geophys. Res.*, 104, 30047-30058.



- 655 21. Kowalczyk P., 2001. Light absorption by yellow substances in Baltic Sea, Doctoral
656 Thesis, Institute of Oceanology Polish Academy of Sciences (in polish).
- 657 22. Kowalczyk P., Kaczmarek S., 1996. Analysis of temporal and spatial variability of
658 “yellow substance” absorption in the Southern Baltic, *Oceanologia*, 38(1), 3-32.
- 659 23. Kowalczyk P., Olszewski J., Darecki M., Kaczmarek S., 2005. Empirical relationships
660 between coloured dissolved organic matter (CDOM) absorption and apparent optical
661 properties in Baltic Sea waters, *Int. J. Rem. Sens.*, 26 (2), 345-370.
- 662 24. Kowalczyk P., Cooper W. J., Whitehead R. F., Durako M. J., Sheldon W., 2003.
663 Characterization of CDOM in an organic rich river and surrounding coastal ocean in
664 the South Atlantic Bight, *Aquat. Sci.*, 65, 381–398.
- 665 25. Kowalczyk P., Stedmon C. A., Markager S., 2006. Modeling absorption by CDOM In
666 the Baltic Sea from season, salinity and chlorophyll, *Mar. Chem.*, 101, 1-11.
- 667 26. Kowalczyk P., Darecki M., Zabłocka M., Górecka I., 2010. Validation of empirical
668 and semi-analytical remote sensing algorithms for estimating absorption by Coloured
669 Dissolved Organic Matter in the Baltic Sea from SeaWiFS and MODIS imagery,
670 *Oceanologia*, 52(2), 171-196.
- 671 27. Kratzer C. R., Brezonik P. L., 1981. A Carlson-type trophic state index for nitrogen
672 in Florida Lakes, *Water Res. Bull.*, 17, 713-715.
- 673 28. Miller, R.L., Belz, M., Del Castillo, C., Trzaska, R., 2002. Determining CDOM
674 absorption spectra in diverse coastal environments using a multiple pathlength, liquid
675 core waveguide system. *Cont. Shelf Res.* 22, 1301–1310.
- 676 29. Moran M.A., Hodson R.E., 1994. Support of bacterioplankton production by dissolved
677 humic substances from three marine environments, *Mar. Ecol. Prog. Ser.*, 110, 241-
678 247.
- 679 30. Morel A., Gentili B., 2009. The dissolved yellow substance and the shades of blue in
680 the Mediterranean Sea, *Biogeosciences*, 6, 2625-2636.
- 681 31. Morel A., Prieur L., 1977. Analysis of variations in ocean color, *Limnol. Oceanogr.*,
682 22(4), 709-722.
- 683 32. Morel A., Claustre H., Gentili B., 2010. The most oligotrophic subtropical zones of
684 the global ocean: similarities and differences in terms of chlorophyll and yellow
685 substance, *Biogeosciences*, 7, 3139-3151.



- 686 33. Morel, A., Gentili, B., Claustre, H., Babin, M., Bricaud, A., Ras, J., Tièche, F., 2007.
687 Optical properties of the “clearest” natural waters. *Limnol. Oceanogr.* 52 (1), 217–
688 229.
- 689 34. Nelson, N.B., Siegel, D.A., 2002. Chromophoric DOM in the open ocean. In: Hansell,
690 D.A., Carlson, C.A. (Eds.), *Biogeochemistry of Marine Dissolved Organic Matter*.
691 Academic Press, San Diego, CA, pp. 547–578.
- 692 35. Organelli E., Bricaud A., Antoine D., Matsuoka A., 2014. Seasonal dynamics of light
693 absorption by chromophoric dissolved organic matter (CDOM) in the NW
694 Mediterranean Sea (BOUSSOLE site), *Deep-Sea Res.*, 91, 72-85.
- 695 36. Pope R. M., Fry E. S., 1997. Absorption spectrum (380-700 nm) of pure water. II
696 Integrating cavity measurements, *Appl. Optics*, 36(33), 8710-8723.
- 697 37. Sartory D. P., Grobbelaar J. U., 1984. Extraction of chlorophyll a from freshwater
698 phytoplankton for spectrophotometric analysis, *Hydrobiologia* 114, 177 – 187.
- 699 38. Sathyendranath S., Prieur L., Morel A., 1989. A three-component model of ocean
700 colour and its application to remote sensing of phytoplankton pigments in coastal
701 waters, *Int. J. Remote Sens.*, 10(8), 1373-1394.
- 702 39. Siegel, D.A., Maritorea, S., Nelson, N.B., Behrenfeld, M.J., McClain, C.R., 2005.
703 Colored dissolved organic matter and its influence on the satellite-based
704 characterization of the ocean biosphere. *Geophys. Res. Lett.* 32, L20605.
705 <http://dx.doi.org/10.1029/2005GL024310>.
- 706 40. Stedmon C., Markager S., 2001. The optics of chromophoric dissolved organic matter
707 (CDOM) in the Greenland Sea: An algorithm for differentiation between marine and
708 terrestrially derived organic matter, *Limnol. Oceanogr.* 46(8), 2087-2093.
- 709 41. Stedmon, C.A., Markager, S., Kaas, H., 2000. Optical properties and signatures of
710 chromophoric dissolved organic Matter (CDOM) in Danish coastal waters. *Estuar.*
711 *Coast. Shelf Sci.* 51, 267–278.
- 712 42. Stramska, M., D. Stramski, R. Hapter, S. Kaczmarek and J. Stoń. 2003. Bio-optical
713 relationships and ocean color algorithms for the north polar region of the Atlantic. *J.*
714 *Geophys. Res.* 108(C5):3143, doi:10.1029/2001JC001195.
- 715 43. Strickland, J. D. H., and T. R. Parsons. 1972. A practical handbook of seawater
716 analyses. Fisheries Research Board of Canada. Ottawa.
- 717 44. Tassan S., 1994. Local algorithms using SeaWiifs data for the retrieval of
718 phytoplankton, pigments, suspended sediment, and yellow substance in coastal waters,
719 *App. Optics*, 33(12), 2369-2378.



- 720 45. Tedetti, M., Charrière, B., Bricaud, A., Para, J., Raimbault, P., Sempère, R., 2010.
721 Distribution of normalized water-leaving radiances at UV and visible wave bands in
722 relation with chlorophyll a and colored detrital matter content in the southeast Pacific.
723 J. Geophys. Res. 115, C02010. <http://dx.doi.org/10.1029/2009JC005289>.
- 724 46. Vodacek A., Blough N. V., DeGrandpre M. D., Peltzer E. T., Nelson R. K., 1997.
725 Seasonal variation of CDOM and DOC in the Middle Atlantic Bight: terrestrial inputs
726 and photooxidation, Limnol. Oceanogr. 42, 674–686.
- 727 47. Wetzel R.G., 2001, Limnology. Lake and River Ecosystems, Third Ed. Academic
728 Press, San Diego, 1006.
- 729 48. Whitehead R.F., de Mora S., 2000, Marine Photochemistry and UV radiation, [in:]
730 Issues in Environmental Science and Technology, Hester, R.E., Harrison R.M. (eds.),
731 Causes and Environmental Implications of Increased UV-B Radiation, Royal Society
732 of Chemistry, 14, 37–60.
- 733 49. Woźniak B., Dera J., 2007. Light Absorption in Sea Water, Springer, New York.
- 734 50. Woźniak S. B., Meler J., Lednicka B., Zdun A., Stoń-Egiert J., 2011. Inherent optical
735 properties of suspended particulate matter in the southern Baltic Sea, Oceanologia,
736 53(3), 691-729.
- 737 51. Ylöstalo, P., K. Kallio, J. Seppälä. 2014. Absorption properties of in-water
738 constituents and their variation among various lake types in the boreal region. Remote
739 Sens. Environ. 148:190-205.
- 740



741 **Table 1.** Dates, number of samples collected and parameters measured during cruises and
 742 field experiments made for this study.

Dates of cruises	Number of samples	Parameters measured	Region
24-31 Aug. 2006	20	$a_{\text{CDOM}}(\lambda)$, <i>Chla</i> , CTD	southern Baltic Proper, Gulf of Gdańsk
24-29 Sept. 2006	12	$a_{\text{CDOM}}(\lambda)$, <i>Chla</i> , CTD	southern Baltic Proper, Gulf of Gdańsk
18-28 Oct. 2006	30	$a_{\text{CDOM}}(\lambda)$, <i>Chla</i> , CTD	southern Baltic Proper, Gulf of Gdańsk, Pomeranian Bay
21-31 March 2007	36	$a_{\text{CDOM}}(\lambda)$, <i>Chla</i> , CTD	southern Baltic Proper, Gulf of Gdańsk, Pomeranian Bay, Szczecin Lagoon
21-31 May 2007	38	$a_{\text{CDOM}}(\lambda)$, <i>Chla</i> , CTD	southern Baltic Proper, Gulf of Gdańsk
20-28 Oct. 2007	26	$a_{\text{CDOM}}(\lambda)$, <i>Chla</i> , CTD	southern Baltic Proper, Gulf of Gdańsk
01-11 March 2008	29	$a_{\text{CDOM}}(\lambda)$, <i>Chla</i> , CTD	southern Baltic Proper, Gulf of Gdańsk, Pomeranian Bay
11-18 April 2008	22	$a_{\text{CDOM}}(\lambda)$, <i>Chla</i> , CTD	southern Baltic Proper, Gulf of Gdańsk
06-14 May 2008	23	$a_{\text{CDOM}}(\lambda)$, <i>Chla</i> , CTD	southern Baltic Proper, Gulf of Gdańsk
01-09 Sept. 2008	26	$a_{\text{CDOM}}(\lambda)$, <i>Chla</i> , CTD	southern Baltic Proper, Gulf of Gdańsk, Pomeranian Bay, Szczecin Lagoon
25-29 Nov. 2008	18	$a_{\text{CDOM}}(\lambda)$, <i>Chla</i> , CTD	Gulf of Gdańsk
04-12 March 2009	14	$a_{\text{CDOM}}(\lambda)$, <i>Chla</i> , CTD	Gulf of Gdańsk, Gotland Basin
15-21 April 2009	29	$a_{\text{CDOM}}(\lambda)$, <i>Chla</i> , CTD	southern Baltic Proper, Gulf of Gdańsk
20-28 May 2009	34	$a_{\text{CDOM}}(\lambda)$, <i>Chla</i> , CTD	southern Baltic Proper, Gulf of Gdańsk, Pomeranian Bay, Szczecin Lagoon
07-16 Sept. 2009	35	$a_{\text{CDOM}}(\lambda)$, <i>Chla</i> , CTD	southern Baltic Proper, Gulf of Gdańsk
06-10 Oct. 2009	21	$a_{\text{CDOM}}(\lambda)$, <i>Chla</i> , CTD	southern Baltic Proper, Gulf of Gdańsk
Dec. 2006 – Sept.	66	$a_{\text{CDOM}}(\lambda)$, <i>Chla</i>	Sopot Pier
April – Dec. 2007	10	$a_{\text{CDOM}}(\lambda)$, <i>Chla</i>	Lake Łebsko



April – Sept. 2008	8	$a_{\text{CDOM}}(\lambda)$, <i>Chla</i>	Lake Łebsko
June – Oct. 2009	9	$a_{\text{CDOM}}(\lambda)$, <i>Chla</i>	Lake Łebsko
March – Dec. 2007	10	$a_{\text{CDOM}}(\lambda)$, <i>Chla</i>	Lake Chotkowskie
Feb. – Sept. 2008	8	$a_{\text{CDOM}}(\lambda)$, <i>Chla</i>	Lake Chotkowskie
April – Nov. 2009	8	$a_{\text{CDOM}}(\lambda)$, <i>Chla</i>	Lake Chotkowskie
March – Dec. 2007	9	$a_{\text{CDOM}}(\lambda)$, <i>Chla</i>	Lake Obłęskie
Feb. – Sept. 2008	8	$a_{\text{CDOM}}(\lambda)$, <i>Chla</i>	Lake Obłęskie
May – Nov. 2009	7	$a_{\text{CDOM}}(\lambda)$, <i>Chla</i>	Lake Obłęskie
All data	556		



744 **Table 2.** Range of variability of the spectral slope S , the coefficient of light absorption by
 745 CDOM for wavelengths $\lambda = 375$ nm and 400 nm, $a_{\text{CDOM}(375)}$ and $a_{\text{CDOM}(400)}$, and
 746 concentrations of chlorophyll a , $Chla$, calculated for the empirical data analysed here.

Study area	range of variability	mean value	SD
S [nm^{-1}]			
Baltic lakes together	0.014 – 0.03	0.022	0.0021
	0.007 – 0.02	0.017	0.0030
	0.007 – 0.03	0.021	0.0022
$a_{\text{CDOM}(375)}$ [m^{-1}]			
Baltic lakes together	0.41 – 7.92	1.61	1.17
	2.11 – 14.16	7.11	3.36
	0.41 – 14.16	2.06	2.17
$a_{\text{CDOM}(400)}$ [m^{-1}]			
Baltic lakes together	0.15 – 4.79	0.997	0.73
	1.28 – 8.85	4.47	2.07
	0.15 – 8.85	1.35	1.41
$Chla$ [mg m^{-3}]			
Baltic lakes together	0.72 – 76.94	8.77	11.61
	1.48 – 118.97	39.11	34.15
	0.72 – 118.97	13.09	19.78

747



748 **Table 3.** Relative errors of empirical model expressed by formula (13) enabling the
749 determination of spectral values of CDOM absorption coefficients
750 ($a_{CDOM}(\lambda)$) at selected wavelengths.

Wavelength [nm]	Arithmetic statistics		Logarithmic statistics			
	systematic error	statistical error	systematic error	standard error factor	statistical error	
	$\langle \varepsilon \rangle$ [%]	σ_ε [%]	$\langle \varepsilon \rangle_g$ [%]	x	σ_+ [%]	σ_- [%]
260	1.47	17.03	0.00	1.19	19.06	-16.01
350	3.13	25.16	-0.01	1.29	29.01	-22.49
440	4.01	29.37	-0.01	1.33	32.71	-24.65
500	6.54	39.43	0.01	1.42	42.45	-29.80
550	11.03	55.07	0.00	1.57	57.40	-36.47
600	19.54	79.13	-0.09	1.83	83.43	-45.48

751 **Table 4.** Relative errors of empirical model expressed by formula (14) enabling the
752 determination of spectral values of CDOM absorption coefficients ($a_{CDOM}(\lambda)$) at
753 selected wavelengths.

Wavelength [nm]	Arithmetic statistics		Logarithmic statistics			
	systematic error	statistical error	systematic error	standard error factor	statistical error	
	$\langle \varepsilon \rangle$ [%]	σ_ε [%]	$\langle \varepsilon \rangle_g$ [%]	x	σ_+ [%]	σ_- [%]
260	0.38	9.11	0.00	1.09	8.94	-8.21
350	0.20	6.43	-0.01	1.07	6.86	-6.42
440	0.42	9.51	0.00	1.09	9.39	-8.59
500	2.21	22.11	0.01	1.23	23.01	-18.71
550	6.24	37.86	0.00	1.42	41.79	-29.47
600	16.61	67.45	-0.01	1.76	75.88	-43.14

754



755 **Table 5.** Relative errors of empirical model expressed by formula dependence (15) and (1)
 756 enabling determination of spectral values of CDOM absorption coefficients
 757 ($a_{CDOM}(\lambda)$) at selected wavelengths.

Wavelength [nm]	Arithmetic statistics		Logarithmic statistics			
	systematic	statistical	systematic	standard	statistical error	
	error	error	error	error factor		
	$\langle \varepsilon \rangle$ [%]	σ_ε [%]	$\langle \varepsilon \rangle_g$ [%]	x	σ_+ [%]	σ_- [%]
260	2.81	14.14	1.82	1.15	15.33	-13.29
350	3.69	4.46	3.59	1.04	4.49	-4.30
440	-14.74	14.13	-15.86	1.18	17.53	-14.92
500	-31.15	22.06	-34.44	1.37	36.54	-26.76
550	-43.73	31.25	-50.93	1.67	67.41	-40.27
600	-36.05	50.48	-50.16	2.01	101.01	-50.25
Kowalczyk et al. 2006						
260	9.32	11.48	8.62	1.13	13.02	-11.52
350	5.14	4.70	5.04	1.05	4.68	-4.47
440	-18.16	13.96	-19.29	1.18	17.90	-15.18
500	-35.34	21.93	-38.71	1.38	38.23	-27.66
550	-47.27	27.17	-53.46	1.65	64.71	-39.29
600	-41.25	46.17	-54.77	2.05	104.97	-51.21

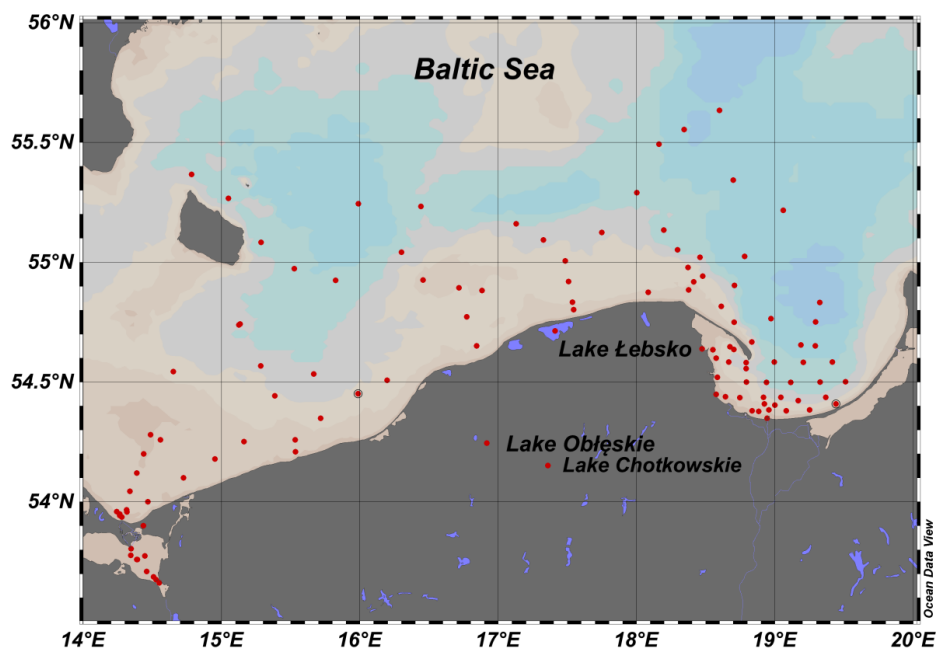
758



759 **Table 6.** Relative errors of Bricaud et al. (1981) and Babin et al. (2003) models enabling
760 determination of spectral values of CDOM absorption coefficients ($a_{CDOM}(\lambda)$) at
761 selected wavelengths.

Wavelength [nm]	Arithmetic statistics		Logarithmic statistics			
	systematic error	statistical error	systematic error	standard error factor	statistical error	
	$\langle \varepsilon \rangle$ [%]	σ_ε [%]	$\langle \varepsilon \rangle_g$ [%]	x	σ_+ [%]	σ_- [%]
Bricaud et al. 1981						
260	-35.74	20.98	-38.79	1.36	35.97	-26.46
350	-6.95	3.64	-7.02	1.04	3.98	-3.82
440	11.10	8.51	10.78	1.08	7.95	-7.37
500	14.24	19.13	12.82	1.17	16.72	-14.32
550	11.21	30.85	7.70	1.28	27.77	-21.74
600	51.80	90.23	33.10	1.64	64.00	-39.03
Babin et al. 2003						
260	-58.45	27.26	-65.30	1.78	77.78	-43.75
350	-33.70	13.85	-35.08	1.23	22.59	-18.43
440	-4.69	4.10	-4.78	1.04	4.45	-4.26
500	12.87	18.23	11.40	1.18	17.77	-15.09
550	26.12	42.51	19.30	1.40	40.12	-28.63
600	92.38	137.52	55.82	1.95	95.05	-48.73

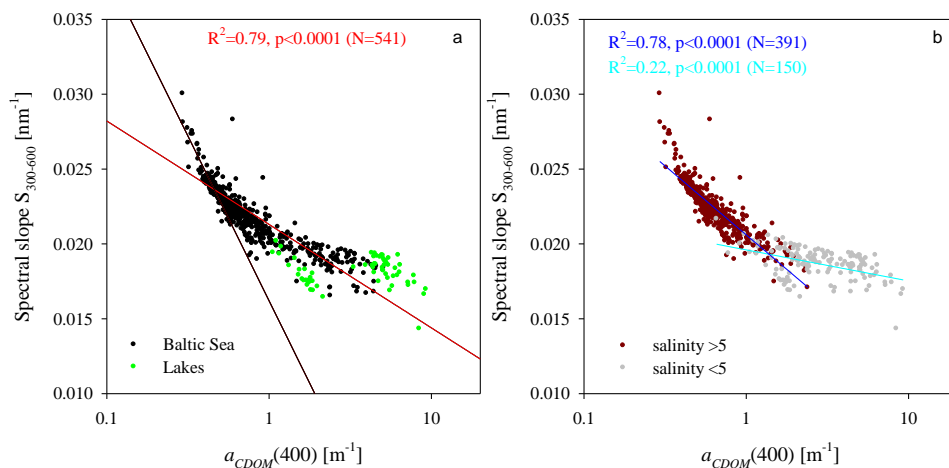
762



763

764 **Figure 1.** Location of the measurement stations in 2006 – 2009

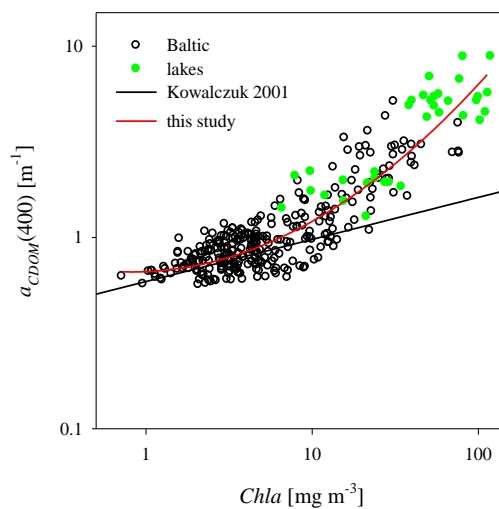
765



766

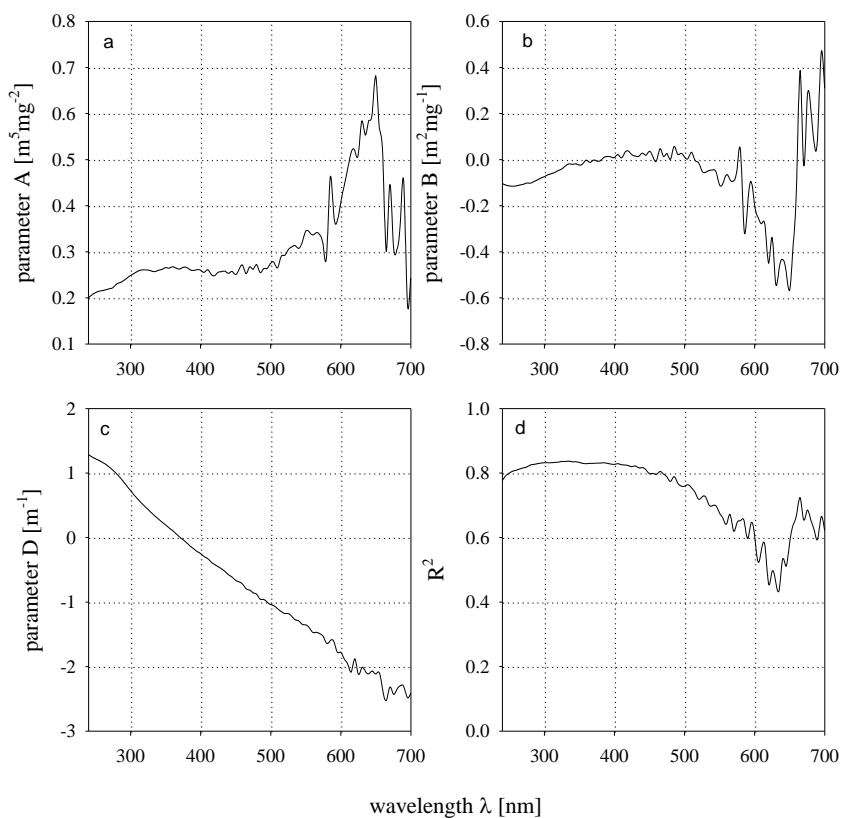
767 **Figure 2.** Relationship between the spectral slope S and the coefficient of light
 768 absorption by CDOM for wavelength 400 nm, $a_{CDOM}(400)$ (a) in the Baltic
 769 (black dots) and lakes (green dots). The black curve is the approximation
 770 obtained by Kowalczyk (2001), the red line represent approximation
 771 expressed by Equation 10; (b) for samples with salinity above 5 (most of the
 772 sea water samples) and with salinity below 5 (samples from lakes, river
 773 mouths, the Szczecin Lagoon). The blue line represent expressed by Equation
 774 (11), and the cyan line by Equation (12).

775



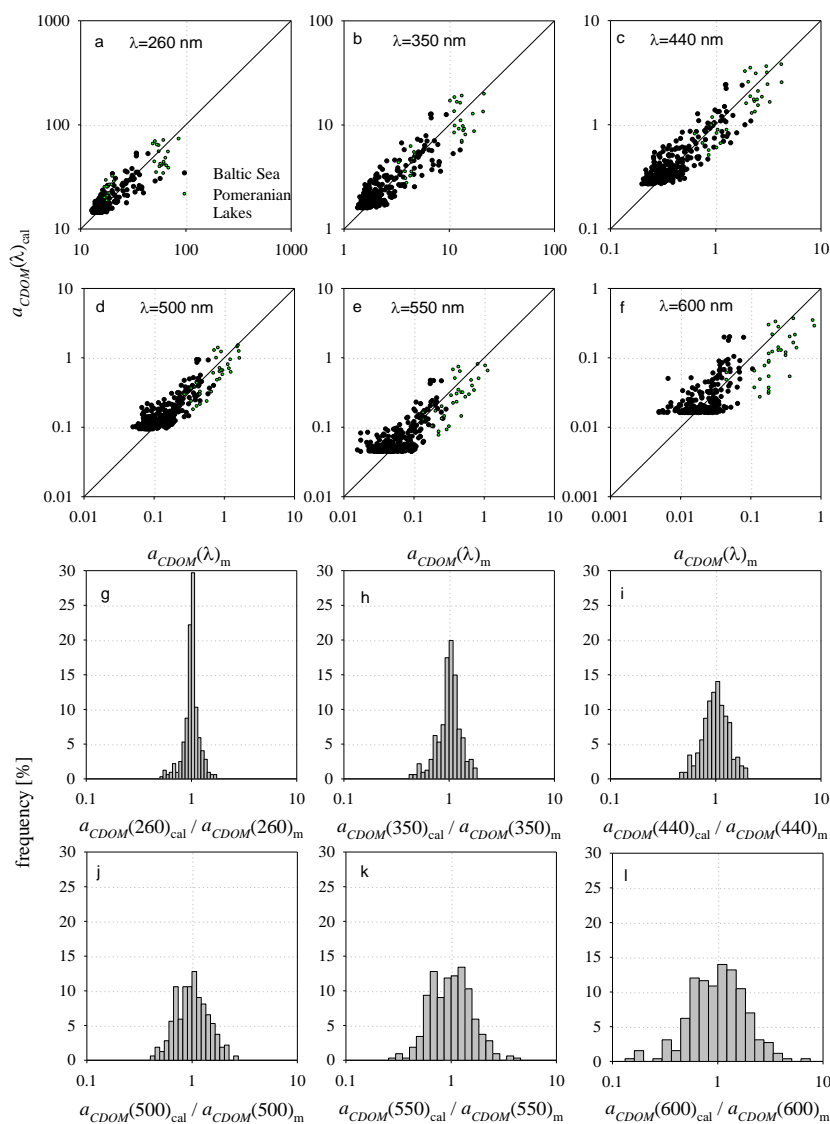
776

777 **Figure 3.** Dependence between coefficients of light absorption by CDOM $a_{CDOM}(400)$ and
778 chlorophyll a concentration. The black line shows the approximation obtained by
779 Kowalczuk (2001) and the red line shows approximation second-degree
780 polynomial in log-log scale.



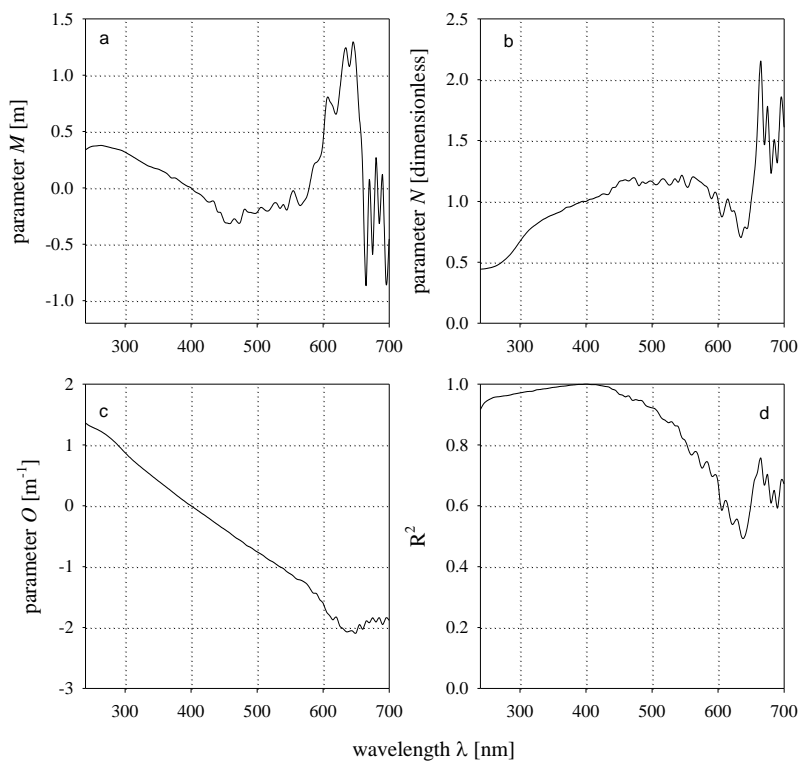
781

782 **Figure 4.** Spectral dependence of the model (expressed by Equation 13) regression
 783 coefficients (panels a and b), free term (panel c) and determination coefficient,
 784 (panel d).



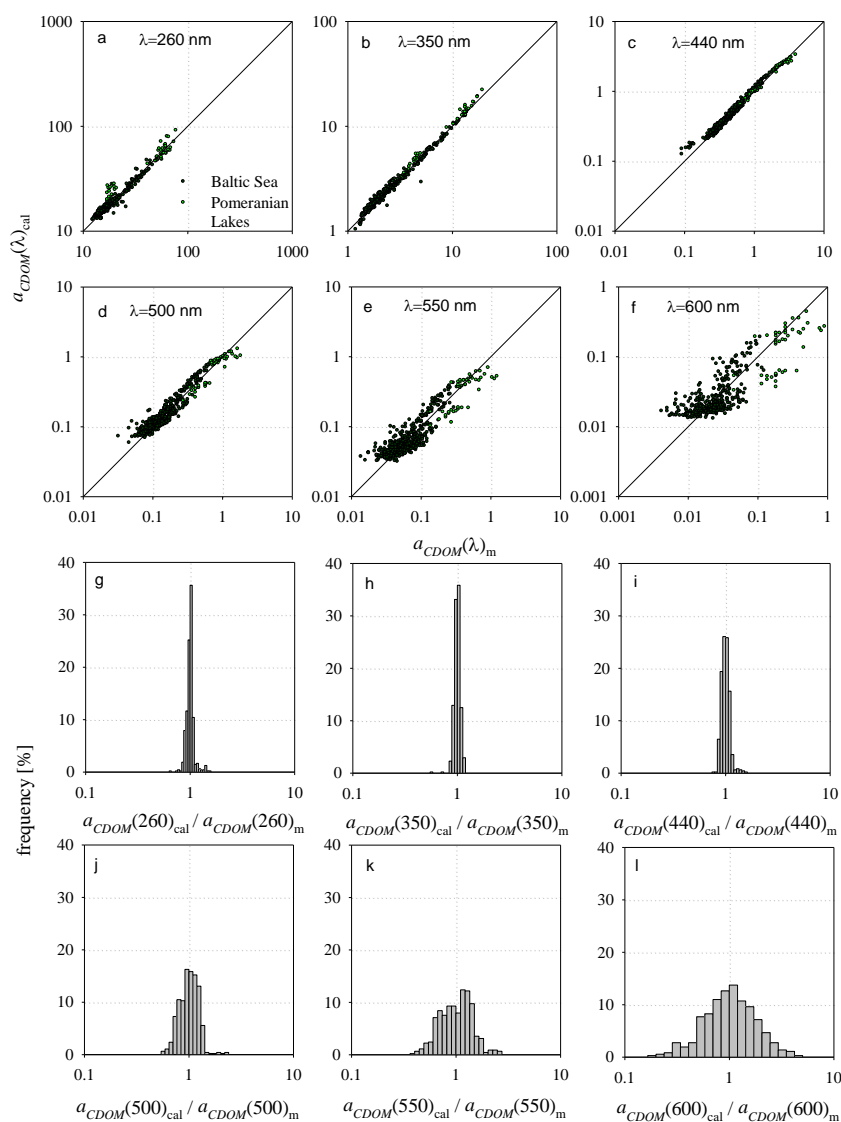
785

786 **Figure 5.** Comparison of light absorption coefficients calculated ($a_{CDOM}(\lambda)_{cal}$) using model
 787 (13) and measured ($a_{CDOM}(\lambda)_m$) in the Baltic (black dots) and Pomeranian lakes
 788 (green dots) for selected wavelengths: (a) 260 nm; (b) 350 nm; (c) 440 nm; (d) 500
 789 nm; (e) 550 nm; (f) 600 nm. The solid line shows the function $a_{CDOM}(\lambda)_{cal} =$
 790 $a_{CDOM}(\lambda)_m$. And the probability density distributions of the ratio of calculated
 791 $a_{CDOM}(\lambda)_{cal}$ to measured $a_{CDOM}(\lambda)_m$ light absorption coefficients for selected
 792 wavelengths: (g) 260 nm; (h) 350 nm; (i) 440 nm; (j) 500 nm; (k) 550 nm; (l)
 793 nm.



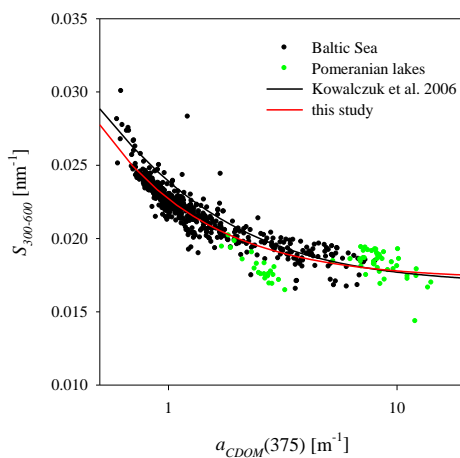
794

795 **Figure 6.** Spectral dependence of the model (expressed by Equation 14) regression
796 coefficients (panels a and b), free term (panel c) and determination coefficient,
797 (panel d).



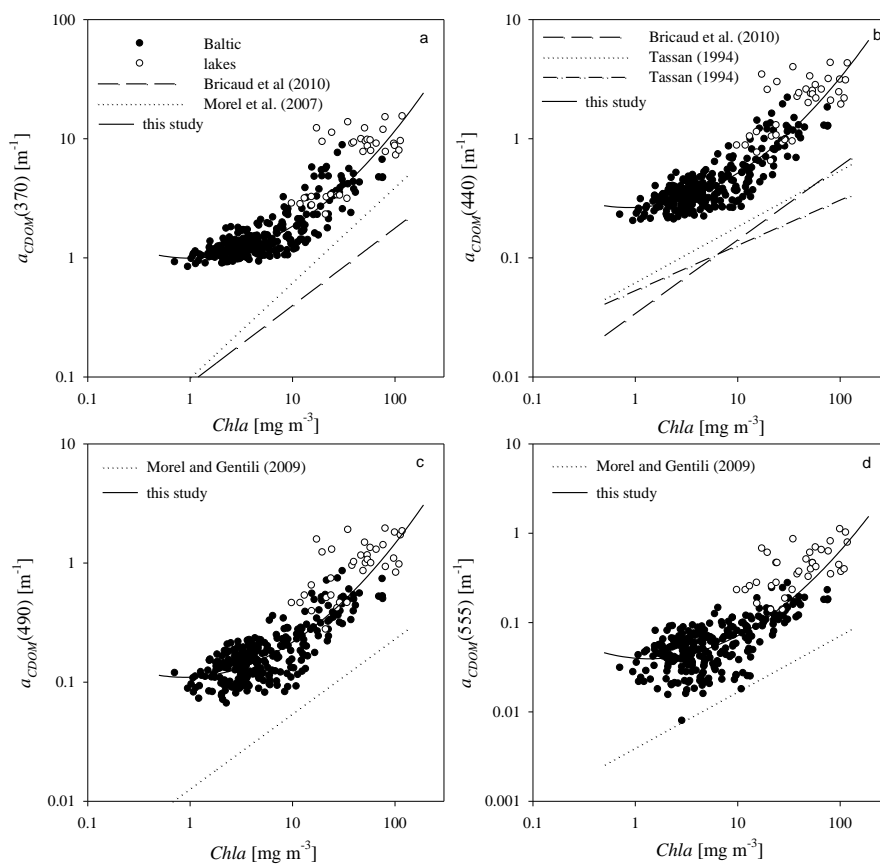
798

799 **Figure 7.** Comparison of light absorption coefficients calculated ($a_{CDOM}(\lambda)_{cal}$) using model
 800 (14) and measured ($a_{CDOM}(\lambda)_m$) in the Baltic (black dots) and Pomeranian lakes
 801 (green dots) for selected wavelengths: (a) 260 nm; (b) 350 nm; (c) 440 nm; (d) 500
 802 nm; (e) 550 nm; (f) 600 nm. The solid line represents the function $a_{CDOM}(\lambda)_{cal} =$
 803 $a_{CDOM}(\lambda)_m$ And the probability density distribution of the ratio of calculated
 804 $a_{CDOM}(\lambda)_{cal}$ to measured $a_{CDOM}(\lambda)_m$ light absorption coefficients for selected
 805 wavelengths: (g) 260 nm; (h) 350 nm; (i) 440 nm; (j) 500 nm; (k) 550 nm; (l) 600
 806 nm.



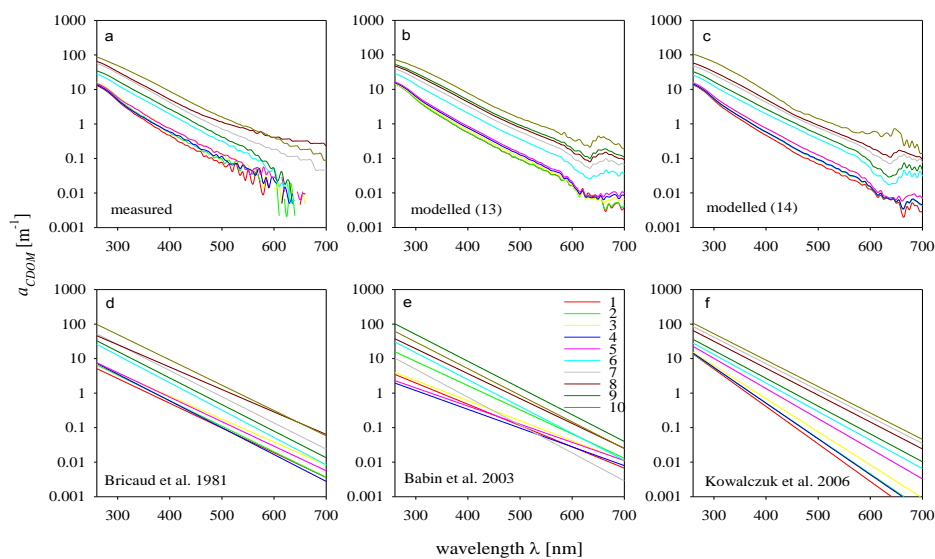
807

808 **Figure 8.** The relationship between the spectral slope coefficient S , and $a_{CDOM(375)}$ in the
809 Baltic (black dots) and lakes (green dots). Black line indicates the model of
810 Kowalczyk et al. (2006) and red one indicates our new approximation (15).



811

812 **Figure 9.** Comparison of relationships between $a_{CDOM}(\lambda)$ and $Chla$ developed in this work
 813 and obtained by different authors for different waters adapted to the data analyzed
 814 in this work.



815

816 **Figure 10.** CDOM light absorption spectra: (a) empirical; (b) calculated using model (13); (c)
817 calculated using model (14); (d) calculated using the model of Bricaud et al. (1981);
818 (e) calculated using the model of Babin et al. (2003); (f) calculated using the model of
819 Kowalczyk et al (2006) for the following concentrations of chlorophyll *a*:

820 (1) $C_a = 0.96 \text{ mg m}^{-3}$, (2) $C_a = 1.31 \text{ mg m}^{-3}$, (3) $C_a = 3.35 \text{ mg m}^{-3}$, (4) 4.94 mg m^{-3} , (5)
821 $C_a = 6.5 \text{ mg m}^{-3}$, (6) $C_a = 28 \text{ mg m}^{-3}$, (7) $C_a = 50 \text{ mg m}^{-3}$, (8) $C_a = 66.43 \text{ mg m}^{-3}$, (9)
822 $C_a = 76.95 \text{ mg m}^{-3}$, (10) $C_a = 119 \text{ mg m}^{-3}$

823



824 **Appendix A.**

825

826 **Table A.** Model parameters for light absorption by CDOM (13) for the wavelength range 240

827 - 700 nm shown for intervals of 5 nm

wave-length [nm]	<i>A</i> [m ⁵ mg ⁻²]	<i>B</i> [m ² mg ⁻¹]	<i>D</i> [m ⁻¹]	R ²	wave-length [nm]	<i>A</i> [m ⁵ mg ⁻²]	<i>B</i> [m ² mg ⁻¹]	<i>D</i> [m ⁻¹]	R ²
<i>1</i>	<i>2</i>	<i>3</i>	<i>4</i>	<i>5</i>	<i>1</i>	<i>2</i>	<i>3</i>	<i>4</i>	<i>5</i>
240	0.200	-0.104	1.286	0.78	475	0.262	0.027	-0.857	0.79
245	0.207	-0.110	1.250	0.79	480	0.272	0.002	-0.880	0.77
250	0.211	-0.114	1.221	0.80	485	0.255	0.057	-0.956	0.79
255	0.214	-0.115	1.195	0.81	490	0.263	0.024	-0.959	0.77
260	0.216	-0.114	1.166	0.81	495	0.264	0.028	-1.003	0.76
265	0.218	-0.110	1.131	0.81	500	0.275	0.010	-1.038	0.76
270	0.220	-0.107	1.090	0.82	505	0.277	0.005	-1.059	0.76
275	0.222	-0.101	1.041	0.82	510	0.265	0.032	-1.105	0.75
280	0.230	-0.102	0.990	0.83	515	0.290	-0.003	-1.147	0.74
285	0.233	-0.095	0.931	0.83	520	0.292	-0.013	-1.177	0.72
290	0.237	-0.088	0.865	0.83	525	0.304	-0.050	-1.178	0.73
295	0.243	-0.080	0.795	0.83	530	0.310	-0.055	-1.221	0.73
300	0.249	-0.074	0.727	0.83	535	0.313	-0.047	-1.275	0.70
305	0.253	-0.066	0.660	0.83	540	0.307	-0.045	-1.292	0.70
310	0.258	-0.061	0.599	0.83	545	0.320	-0.054	-1.345	0.70
315	0.260	-0.055	0.541	0.83	550	0.344	-0.110	-1.354	0.68
320	0.261	-0.047	0.487	0.83	555	0.344	-0.101	-1.398	0.66
325	0.261	-0.040	0.435	0.84	560	0.337	-0.065	-1.470	0.64
330	0.258	-0.027	0.382	0.84	565	0.341	-0.087	-1.468	0.67
335	0.257	-0.019	0.332	0.84	570	0.337	-0.091	-1.491	0.62
340	0.260	-0.020	0.286	0.84	575	0.314	-0.040	-1.537	0.65
345	0.262	-0.018	0.238	0.84	580	0.291	0.036	-1.641	0.65
350	0.266	-0.024	0.196	0.83	585	0.462	-0.307	-1.597	0.65
355	0.265	-0.018	0.150	0.83	590	0.382	-0.195	-1.612	0.60
360	0.268	-0.022	0.108	0.83	595	0.367	-0.095	-1.776	0.65
365	0.265	-0.012	0.059	0.83	600	0.405	-0.198	-1.778	0.61
370	0.263	-0.002	0.008	0.83	605	0.444	-0.251	-1.886	0.52
375	0.266	-0.007	-0.035	0.83	610	0.480	-0.278	-1.963	0.57
380	0.266	-0.004	-0.081	0.83	615	0.516	-0.288	-2.083	0.57
385	0.261	0.009	-0.131	0.83	620	0.520	-0.450	-1.879	0.46
390	0.260	0.014	-0.174	0.83	625	0.510	-0.337	-2.118	0.50
395	0.261	0.012	-0.216	0.83	630	0.584	-0.538	-2.015	0.46
400	0.260	0.009	-0.248	0.83	635	0.553	-0.471	-2.075	0.44
405	0.255	0.022	-0.294	0.83	640	0.585	-0.434	-2.110	0.53
410	0.261	0.008	-0.326	0.83	645	0.600	-0.487	-2.069	0.51



415	0.252	0.032	-0.379	0.83	650	0.682	-0.567	-2.115	0.59
420	0.248	0.037	-0.418	0.82	655	0.572	-0.371	-2.096	0.64
425	0.255	0.021	-0.451	0.82	660	0.512	-0.099	-2.375	0.67
430	0.257	0.016	-0.486	0.82	665	0.301	0.387	-2.524	0.72
435	0.258	0.015	-0.529	0.82	670	0.446	-0.024	-2.320	0.66
440	0.253	0.028	-0.577	0.82	675	0.319	0.264	-2.428	0.69
445	0.258	0.019	-0.614	0.81	680	0.305	0.224	-2.352	0.66
450	0.251	0.036	-0.662	0.80	685	0.360	0.072	-2.297	0.62
455	0.262	0.011	-0.688	0.80	690	0.452	0.103	-2.314	0.60
460	0.271	-0.005	-0.723	0.80	695	0.191	0.466	-2.481	0.67
465	0.253	0.048	-0.795	0.81	700	0.243	0.310	-2.412	0.62
470	0.267	0.014	-0.815	0.80					

828

829 **Table B.** Parameters of the model of light absorption by CDOM (14) for the wavelength
 830 range 240 - 700 nm, shown for intervals of 5 nm

wave- length [nm]	<i>M</i> [m ⁵ mg ⁻²]	<i>N</i> [m ² mg ⁻¹]	<i>O</i> [m ⁻¹]	R ²	wave- length [nm]	<i>M</i> [m ⁵ mg ⁻²]	<i>N</i> [m ² mg ⁻¹]	<i>O</i> [m ⁻¹]	R ²
1	2	3	4	5	1	2	3	4	5
240	0.337	0.444	1.360	0.92	475	-0.300	1.184	-0.572	0.95
245	0.356	0.445	1.323	0.94	480	-0.195	1.129	-0.613	0.95
250	0.369	0.450	1.294	0.95	485	-0.211	1.159	-0.657	0.95
255	0.372	0.455	1.269	0.95	490	-0.217	1.147	-0.682	0.93
260	0.375	0.463	1.243	0.96	495	-0.226	1.163	-0.720	0.93
265	0.376	0.474	1.213	0.96	500	-0.218	1.163	-0.756	0.92
270	0.370	0.490	1.177	0.96	505	-0.176	1.138	-0.787	0.92
275	0.363	0.511	1.136	0.96	510	-0.187	1.150	-0.823	0.90
280	0.355	0.535	1.091	0.96	515	-0.206	1.183	-0.867	0.89
285	0.348	0.562	1.042	0.96	520	-0.188	1.174	-0.901	0.88
290	0.340	0.596	0.988	0.97	525	-0.140	1.137	-0.929	0.87
295	0.332	0.633	0.930	0.97	530	-0.139	1.149	-0.969	0.88
300	0.317	0.672	0.873	0.97	535	-0.182	1.186	-1.005	0.86
305	0.300	0.709	0.819	0.97	540	-0.148	1.158	-1.033	0.86
310	0.283	0.743	0.767	0.98	545	-0.197	1.215	-1.082	0.83
315	0.265	0.771	0.718	0.98	550	-0.092	1.150	-1.116	0.82
320	0.247	0.794	0.673	0.98	555	-0.025	1.119	-1.155	0.79
325	0.229	0.813	0.628	0.98	560	-0.097	1.192	-1.204	0.77
330	0.212	0.833	0.584	0.98	565	-0.157	1.195	-1.217	0.78
335	0.195	0.851	0.541	0.98	570	-0.126	1.174	-1.243	0.76
340	0.185	0.865	0.497	0.99	575	-0.081	1.154	-1.282	0.73
345	0.174	0.880	0.454	0.99	580	0.036	1.130	-1.355	0.74
350	0.167	0.890	0.411	0.99	585	0.187	1.101	-1.434	0.74
355	0.154	0.902	0.370	0.99	590	0.227	1.022	-1.444	0.70



360	0.139	0.913	0.328	0.99	595	0.267	1.075	-1.543	0.70
365	0.119	0.928	0.286	0.99	600	0.420	1.009	-1.601	0.68
370	0.089	0.950	0.244	0.99	605	0.774	0.876	-1.742	0.59
375	0.089	0.955	0.200	1.00	610	0.771	0.937	-1.804	0.61
380	0.073	0.965	0.157	1.00	615	0.719	1.020	-1.873	0.60
385	0.050	0.979	0.115	1.00	620	0.656	0.924	-1.827	0.54
390	0.030	0.990	0.076	1.00	625	0.853	0.918	-1.969	0.55
395	0.014	1.001	0.035	1.00	630	1.122	0.784	-2.016	0.55
400	0.000	1.000	0.000	1.00	635	1.238	0.704	-2.069	0.50
405	-0.029	1.015	-0.038	1.00	640	1.078	0.787	-2.061	0.50
410	-0.046	1.021	-0.075	1.00	645	1.293	0.784	-2.060	0.54
415	-0.063	1.033	-0.115	1.00	650	1.090	0.999	-2.088	0.61
420	-0.092	1.042	-0.151	1.00	655	0.620	1.229	-1.952	0.68
425	-0.122	1.060	-0.190	0.99	660	0.130	1.655	-2.029	0.71
430	-0.123	1.059	-0.228	0.99	665	-0.868	2.149	-1.893	0.76
435	-0.125	1.063	-0.269	0.99	670	0.075	1.468	-1.922	0.67
440	-0.210	1.111	-0.307	0.98	675	-0.590	1.782	-1.839	0.70
445	-0.221	1.118	-0.346	0.98	680	0.268	1.233	-1.910	0.61
450	-0.297	1.161	-0.382	0.97	685	-0.316	1.508	-1.839	0.65
455	-0.312	1.171	-0.419	0.96	690	0.117	1.321	-1.951	0.59
460	-0.314	1.177	-0.458	0.96	695	-0.832	1.847	-1.843	0.68
465	-0.275	1.169	-0.503	0.96	700	-0.453	1.610	-1.882	0.67
470	-0.302	1.190	-0.540	0.95					